JOURNAL OF GEOPHYSICAL RESEARCH, VOL. 104, NO. D6, PAGES 6377–6402, MARCH 27, 1999

Observed and model-simulated diurnal cycles of precipitation over the contiguous United States

Aiguo Dai, Filippo Giorgi,[1] and Kevin E. Trenberth

National Center for Atmospheric Research, Boulder, Colorado

Abstract. We analyzed diurnal variations in precipitation, surface pressure, and atmospheric static energy over the United States from observations and NCAR regional climate model (RegCM) simulations. Consistent with previous studies, the mean (1963-1993) pattern of the diurnal cycle of summer U.S. precipitation is characterized by late afternoon maxima over the Southeast and the Rocky Mountains and midnight maxima over the region east of the Rockies and the adjacent plains. Diurnal variations of precipitation is weaker in other seasons, with early to late morning maxima over most of the United States in winter. The diurnal cycle in precipitation frequency accounts for most of the diurnal variations, while the diurnal variations in precipitation intensity are small. The broad pattern of the diurnal cycle of summer precipitation is fairly stable, but the interannual variability in the diurnal cycle of winter precipitation is large. The diurnal cycle of July convective available potential energy (CAPE) is dominated by a solar driven march of a high-CAPE (2-4 kJ kg^{-1}) tongue moving from the Southeast into the Northwest, with maximum values in the late afternoon to early evening over most of the United States. The solar driven diurnal and semidiurnal cycles of surface pressure result in significant large-scale convergence over most of the western United States during the day and over the region east of the Rockies at night. The diurnal cycle of low-level large-scale convergence suppresses daytime convection and favors nighttime moist convection over the region east of the Rockies and the adjacent plains. The nocturnal maximum in the region east of the Rockies is also enhanced by the eastward propagation of late afternoon thunderstorms generated over the Rockies. Over the Southeast and the Rockies, both the static instability and the surface convergence favor afternoon moist convection in summer, resulting in very strong late afternoon maxima of precipitation over these regions. RegCM simulations of 1993 summer precipitation with three different cumulus convection schemes (Grell, Kuo, CCM3) all had deficiencies in capturing the broad pattern of the diurnal cycle of precipitation over the United States. The model also overestimated precipitation frequency and underestimated precipitation intensity. The simulated diurnal cycles of surface pressure and CAPE were weak compared to observations. All the schemes produced too much cloudiness over the Southeast for July 1993 which reduced surface solar radiation and thus daytime peak warming at the surface. The model's criteria for onset of moist convection appear to be too weak, so moist convection in the model starts too early and occurs too often with all the three schemes.

1. Introduction

Precipitation does not occur all the time, yet it is common to consider only total amounts. Just as important is the frequency and intensity of precipitation. The diurnal cycle of precipitation frequency and intensity has large effects on surface hydrology (runoff, evaporation). For example, rainfall during the afternoon is likely to be evaporated more quickly than at night. Diurnal variations of precipitation can also modulate the surface temperature range [*Dai et al.*, 1998] and are closely related to the diurnal cycles of atmospheric moist convection and cloudiness, which greatly affects the solar and long-wave radiation at the surface. Documentation of the diurnal variability of precipitation over the contiguous United States has been the topic of a large number of studies [e.g., *Wallace*, 1975; *Schwartz*

[1]Now at Physics of Weather and Climate Group, The Abdus Salam International Centre for Theoretical Physics, Trieste, Italy.

Paper number 98JD02720.
0148-0227/99/98JD-02720$09.00

and Bosart, 1979; *Balling*, 1985; *Easterling and Robinson*, 1985; *Englehart and Douglas*, 1985; *Riley et al.*, 1987; *Landin and Bosart*, 1989; *Tucker*, 1993; *Higgins et al.*, 1996]. These studies have shown a distinctive geographical pattern of precipitation diurnal variations during summer which is characterized by a strong midnight to early morning maximum (of precipitation frequency) over the region east of the Rockies and the Great Plains and a strong late afternoon maximum over the southeastern and western United States. The diurnal cycle of precipitation is relatively weak during other seasons, with small peaks usually in the morning over most of the United States [*Wallace*, 1975; *Riley et al.*, 1987; *Landin and Bosart*, 1989]. However, most of these studies have not examined the diurnal cycle in intensity and amounts.

A number of physical mechanisms have been proposed to explain the diurnal cycle patterns. *Wallace* [1975] suggested that the familiar coastal land and sea breeze circulations, the solar heating over sloping terrain, and diurnal changes in frictional drag of the planetary boundary layer may induce diurnal variations in low-level convergence that largely controls the timing of convective precipitation during summer. *Riley et al.* [1987] argued, based on the phase transition in the diurnal cycle of precipitation, that heavy summer nocturnal precipitation systems over the Great Plains cannot be explained solely by the eastward propagation of mountain-generated systems from the previous afternoon. Others have linked the nocturnal precipitation maxima over the Great Plains to the diurnal cycle of the large-scale circulation over the region east of the Rockies such as the low-level jet [*Bleeker and Andre*, 1951; *Hering and Borden*, 1962; *Pitchford and London*, 1962; *Reiter and Tang*, 1984; *Nicolini et al.*, 1993]. Over the Florida peninsula, sea-breeze-induced convergence appears to contribute to the convective rainfall there [*Burpee*, 1979; *Schwartz and Bosart*, 1979].

The goal of this study is to (1) provide a more comprehensive description of the spatial and seasonal patterns of the diurnal cycle of precipitation over the contiguous United States, including not only frequency but also intensity and amounts; (2) examine the relative roles of the thermally driven atmospheric tides in pressure fields [*Chapman and Lindzen*, 1970] and static instability in the control of the timing of convective precipitation during summer; and (3) analyze the NCAR regional climate model (RegCM) simulated diurnal cycle of precipitation to illuminate the processes involved and diagnose the model deficiencies.

Higgins et al. [1996] created a gridded 31-year (1963-1993) data set of hourly precipitation from quality-controlled station records at approximately 2500 United States stations, which greatly exceeds the number of stations used in previous analyses. This data set provided us the opportunity to document the diurnal cycle of precipitation over the United States more comprehensively. It should be emphasized, however, that the diurnal cycle of precipitation intensity and amount derived from the gridded (i.e., averaged) data is likely to have smaller amplitudes than those at individual stations. On the other hand, the gridded data facilitate the comparison with model results.

In previous studies, physical mechanisms for the diurnal cycle of precipitation are often proposed on the basis of spatial or seasonal characteristics of the diurnal cycle itself. Although diurnal variations of large-scale convergence over the region east of the Rockies were examined [*Bleeker and Andre*, 1952; *Hering and Borden*, 1962; *Pitchford and London*, 1962; *Reiter and Tang*, 1984], their relevance to the diurnal cycle of precipitation over the central United States has not been well established because the convergence derived from large-scale circulation fields can result from moist convection itself. It is well known that thermal heating (through atmospheric ozone, water vapor, and the ground) by the Sun generates considerable diurnal and semidiurnal cycles (called atmospheric tides) in atmospheric temperature, pressure, and wind fields [*Lindzen*, 1967; *Wallace and Hartranft*, 1969; *Haurwitz and Cowley*, 1973; *Trenberth*, 1977; Dai and Wang, Diurnal and semidiurnal tides in global surface pressure fields, submitted to *Journal of the Atmospheric Sciences*, 1998]. The semidiurnal tide is largely a global propagating mode, while the diurnal tide is more local. The diurnal cycle of surface winds, such as sea breezes, results largely from pressure gradients set up by atmospheric tides. For example, *Deser and Smith* [1998] are able to reproduce much of the semidiurnal variation (main component) of near-surface zonal winds over the tropical Pacific Ocean using the semidiurnal component of surface pressure fields.

In this study we analyze the thermally driven diurnal and semidiurnal cycles in surface pressure fields and the associated continental-scale convergence. We also examine the diurnal cycles of atmospheric static instability and the low-level circulation fields using the National Centers for Environmental Predictions/National Center for Atmospheric Research (NCEP/NCAR) reanalysis. Our results show that the diurnal cycle of the thermally driven tides in the atmosphere largely determines the timing of summer moist convective precipitation over the United States.

The diurnal cycle of precipitation has not been analyzed in most of the climate model simulations, despite the fact that *Wilson and Mitchell* [1986] have demonstrated that the simulation of climate in a global climate model (GCM) will be degraded if the diurnal cycle is not resolved adequately. *Chen et al.* [1996] examined hourly precipitation over the United States in the NCAR Community Climate Model (CCM, version 2) simulations and found that the model precipitation frequency is much too high, while the model intensity is much too low compared with observations. Many models appear to have problems in simulating the diurnal variations of precipitation (e.g., the European Centre for Medium-Range Weather Forecast (ECMWF) model

does not rain at the right time, and our preliminary analyses of the CCM (version 3) and NASA GISS GCM precipitation revealed large model deficiencies). In this study we analyze the diurnal cycle of precipitation in the high-resolution RegCM simulations of summer precipitation over the United States with different cumulus convection schemes and provide suggestions for future model improvements.

In section 2 we describe the various data sets and the analysis methods we used in this study, including a summary of the model simulations. In section 3 we present the results from the analysis of observational data. The model results are discussed in section 4. In section 5 we summarize the results and discuss the implications.

2. Data and Analysis Methods

2.1. Hourly Precipitation Data

The observational data of hourly precipitation used in this study are from *Higgins et al.* [1996], in the form of a gridded (2.5° longitude by 2.0° latitude) data set derived from quality-controlled station records from about 2500 United States stations. It covers the period from January 1, 1963 to December 31, 1993 (data for 1994 are incomplete and thus not used in this study). More details, including the gridding method, can be found in the work of *Higgins et al.* [1996]. Although hourly precipitation is extremely variable in space and time, the gridded data can still be used for examining the large-scale features of precipitation diurnal cycle over the United States and for evaluating model precipitation fields.

We first computed the seasonal averages of hourly precipitation amount, frequency, and intensity and then applied the following three methods to analyze the diurnal cycle in these quantities: (1) to fit the hourly data with multiple harmonics and determine the diurnal amplitude and phase based on the 24-hour harmonic, (2) to fit the hourly data with multiple harmonics and determine the maximum and preferred time of occurrence (i.e., the mean solar local time (LST) at which the maximum value occurs) based on the fitted curve, and (3) to directly examine the hourly data to determine the maximum and the preferred time. Method 1 is similar to that used by *Wallace* [1975]. Tests showed that the three methods produce comparable results in terms of capturing the maximum and the preferred time. In this paper we present results from only the third method, mainly because diurnal curves of precipitation differ greatly from simple harmonics (compare Figure 2). We temporally smoothed the hourly data by using a 3-point running mean prior to the diurnal analysis which makes the spatial patterns smoother (the magnitude of the amplitude changes only slightly). We also normalized the amplitude (equal to the maximum minus the 24-hour mean) by the 24-hour mean, as in the *Wallace* [1975] and other studies, and present the normalized amplitude as a percentage. For instance, a normalized amplitude of 50% would mean that the maximum value (which could be precipitation amount, frequency, or intensity) is 1.5 times the 24-hour mean. The normalized amplitude does not work well in the cases when the 24-hour mean is very small, such as in California during summer. Nevertheless, it provides a measure of the magnitude of the diurnal cycle relative to the 24-hour mean. We present the amplitude and the preferred time using vector plots in a fashion similar to those of *Higgins et al.* [1996]. The same analysis method was applied to the model-simulated hourly precipitation data.

We also tried to categorize the hourly data as light and heavy precipitation using various thresholds but failed to find significant differences between the categorized precipitation, presumably because the gridded (i.e., spatially averaged) hourly precipitation differs from station records so that conventional definitions of light (< 2.5 mm/h) and heavy (> 2.5 mm/h) precipitation [*Wallace*, 1975] are not applicable. We focus our analysis on the amount, frequency, and intensity of measurable precipitation (defined here as > 0.1 mm/h for the gridded precipitation).

2.2. Surface Pressure and Atmospheric Circulation Data

The newly released 3 hourly surface pressure data set from the reanalysis generated with version 1 of the Goddard Earth Observing System (GEOS 1) Data Assimilation System [*Schubert et al.*, 1995; *Wu et al.*, 1997] was used to calculate the diurnal (S_1) and semidiurnal (S_2) components in surface pressure fields. The data set covers a 15-year period (1980-1994) and is on a global grid of 2.5° longitude by 2.0° latitude. The spatial patterns of S_1 and S_2 derived from this data set are highly comparable with those of *Haurwitz and Cowley* [1973] and *Trenberth* [1977], suggesting that the data set is useful for our purpose (see *Dai and Wang* [1998] for more details).

The diurnal curves of surface pressure are fairly smooth [*Trenberth*, 1977] and can be fitted with high precision by diurnal and semidiurnal harmonics. We derived S_1 and S_2 by fitting the data with the two harmonics. Since the data are averaged values over a 3-hour period, the calculated amplitudes of S_1 and S_2 need to be multiplied by a factor (F) to obtain the real amplitudes that one would get from using instantaneous values. The factor $F = \frac{\omega \Delta t}{2\sin(\omega \Delta t/2)}$, where ω = angular frequency and Δt = averaging time period (= 3 hours), can be easily derived by averaging a sine function over a given period. $F = 1.0262$ for S_1 and 1.1107 for S_2, where $\omega = 2\pi/24$ for S_1 and $2\pi/12$ for S_2.

We used the linearized horizontal wind (u and v) equations [*Holton*, 1979] to compute the divergence on sigma surfaces induced by the diurnal and semidiurnal variations in the surface pressure field (p). Linearization allowed us to derive the following ordinary differential equation for divergence ($D = \nabla \bullet \mathbf{V}$) which leads to a set of linear algebra equations when substituting

the harmonics of S_1 and S_2 for p and the diurnal and semidiurnal harmonics for D:

$$\frac{\partial^2 D}{\partial t^2}+2k\frac{\partial D}{\partial t}+(k^2+f^2)D+\frac{1}{\rho_o}\nabla^2\frac{\partial p}{\partial t}+\frac{k}{\rho_o}\nabla^2 p=0 \quad (1)$$

where f = Coriolis parameter, ρ_o = air density at the surface (assumed constant), and k = linear friction coefficient ($-ku$ and $-kv$ were added to the right side of u and v equations). Tests showed that D is insensitive to k, and a value of 1.0 x 10^{-5} s^{-1} is adopted for k. It should be emphasized that the calculated divergence using equation (1) is only an approximate estimate of the pressure-induced divergence field.

We used the 6 hourly NCEP/NCAR reanalysis data (temperature and humidity profiles of individual years) [*Kalnay et al.*, 1996] to calculate convective available potential energy (CAPE) (defined as CAPE = $\int_z(T_{vp}-T_{va})d\ln p(z)$, where T_{vp} and T_{va} are virtual temperatures of an air parcel and the environment, respectively, $p(z)$ is the pressure at height z, and the integration is from the first layer (sigma=0.995) up to about 200 mbar). CAPE has been widely used as a measure of the static instability of the atmosphere [e.g., *Williams and Renno*, 1993; *Fu et al.*, 1994], and CAPE$\geq$ 1 kJ kg^{-1} is usually considered enough for moist convection [*Lucas et al.*, 1994]. We employ it here as an indicator of local static instability under mean July conditions. We also examine low-level horizontal and vertical winds using the reanalysis data. The 6 hourly data are not really adequate for analyses of diurnal cycles but nevertheless provide us some useful information on the day-night differences. The moisture fields of the NCEP/NCAR reanalysis were found to have large negative biases in the tropics [*Trenberth and Guillemot*, 1998]. Nevertheless, the reanalysis appears to be acceptable over the United States where observations are dense.

2.3. Model Simulations

The regional climate model (RegCM) developed at NCAR and the precipitation and cumulus convection schemes used in the model are described by *Giorgi and Shields* [this issue]. Here we briefly summarize the relevant aspects of the simulations.

A simplified version of the explicit moisture scheme [*Hsie et al.*, 1984] is used to calculate resolvable-scale ($\geq$ 60 km) precipitation and cloudiness in the model. The model calculates cloud water and allows it to convert into rainwater, which is immediately precipitated out, via a Kessler-type autoconversion. Fractional cloud cover is specified as 0.75 whenever there is cloud water inside a grid box, which is 60 km x 60 km. The calculated cloud water and fractional cloud cover are directly used in the radiation transfer calculations.

The model has been run separately with three different cumulus convection schemes. The first one is a scheme developed by *Grell* [1993] (referred to as the Grell scheme in this paper). In this scheme, the mass flux of updraft (m_b) and downdraft is constant with height, and rainfall is given by $R = I_1 m_b(1-\beta)$, where I_1 is the amount of condensate integrated over the whole depth of the updraft and β varies between 0.25 and 0.50 as a function of the vertical wind shear. An *Arakawa and Schubert* [1974] type closure is used to calculate m_b.

The second convection scheme is a Kuo-type scheme (referred to as the Kuo scheme) described by *Anthes et al.* [1987]. In this scheme, precipitation is initiated when the moisture convergence in a column exceeds a given threshold and the vertical sounding is unstable. A fraction of the total moisture convergence precipitates, depending on the mean columnar relative humidity, while the remaining fraction is redistributed throughout the column.

The third convection scheme (referred to as the CCM3 scheme) is described by *Zhang and McFarlane* [1995] and is used in the NCAR Community Climate Model version 3 [*Kiehl et al.*, 1996]. It is a mass flux scheme in which the effects of cumulus convection are represented in terms of ensembles of cloud updrafts and downdrafts. Deep convection occurs when the atmosphere is locally conditionally unstable in the lower troposphere. Cloud water content (l) is calculated and allowed to convert to rainwater, which is immediately rained out. The total precipitation is given by $P = c_0\int_z M_u l dz$, where M_u is the ensemble cloud updraft mass flux and c_0 is a constant.

The simulations (time step = 200 s, grid size = 60 km with 14 sigma levels in the vertical) begin on March 1, 1993, and end on February 28, 1996, and cover a domain (Figure 1) encompassing the whole continental United States. The time-dependent lateral boundary conditions are provided from the ECMWF operational analyses. The simulated diurnal cycles of precipitation are comparable for the 3 years and are weak in winter. Our analysis, which was done using the hourly data saved during the simulations, will focus on 1993 summer precipitation.

2.4. Cloud Cover and Surface Solar Irradiance Data

In diagnosing the model deficiencies, we used daytime surface observations of cloud cover and surface solar downward flux data for July 1993 to evaluate the model. We extracted the cloud cover records from about 680 United States stations from the NCAR data archives (DS464.0) and averaged all stations within each 1^o x 1^o grid box and then linearly interpolated the data onto a coarser grid. The surface solar fluxes are from *Zhang et al.* [1995] and are calculated on the basis of observations of the properties of clouds, the atmosphere, and the surface. The fluxes have an uncertainty of about 15-25 W m^{-2} [*Rossow and Zhang*, 1995] and a year-to-year variability (s.d.) of 10-50 W m^{-2} over the United States. The data are available only for 1985-1988. We used the averaged values for the 4-year period in the comparison

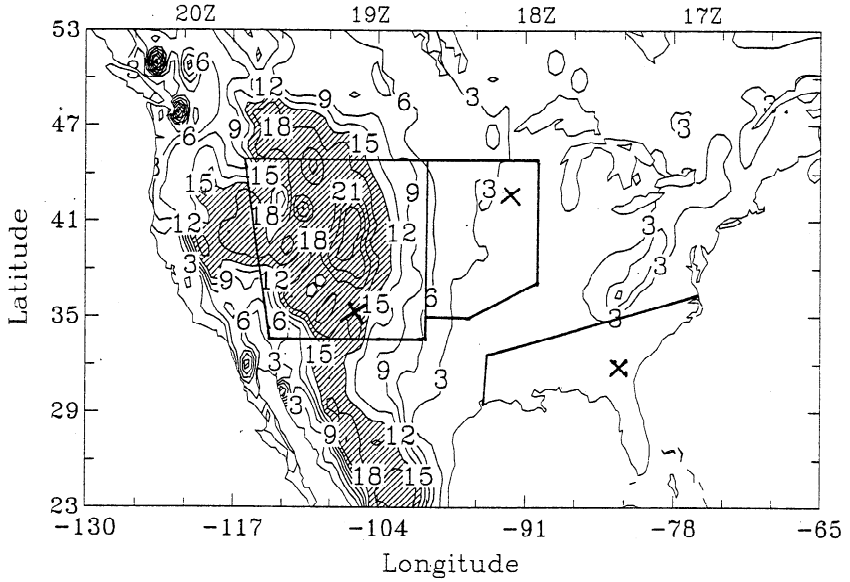

Figure 1. Approximate domain of simulation in the NCAR regional climate model (RegCM). Also shown are contour lines of topography (in 100 m, areas over 1500 m are hatched), the locations (marked by a cross) of the three grid boxes referred to in Figure 2, and the approximate definition of the southeastern United States, the Rocky Mountains, and the region east of the Rockies and the adjacent plains used in this study. The Greenwich time corresponding to local noontime is shown at the top.

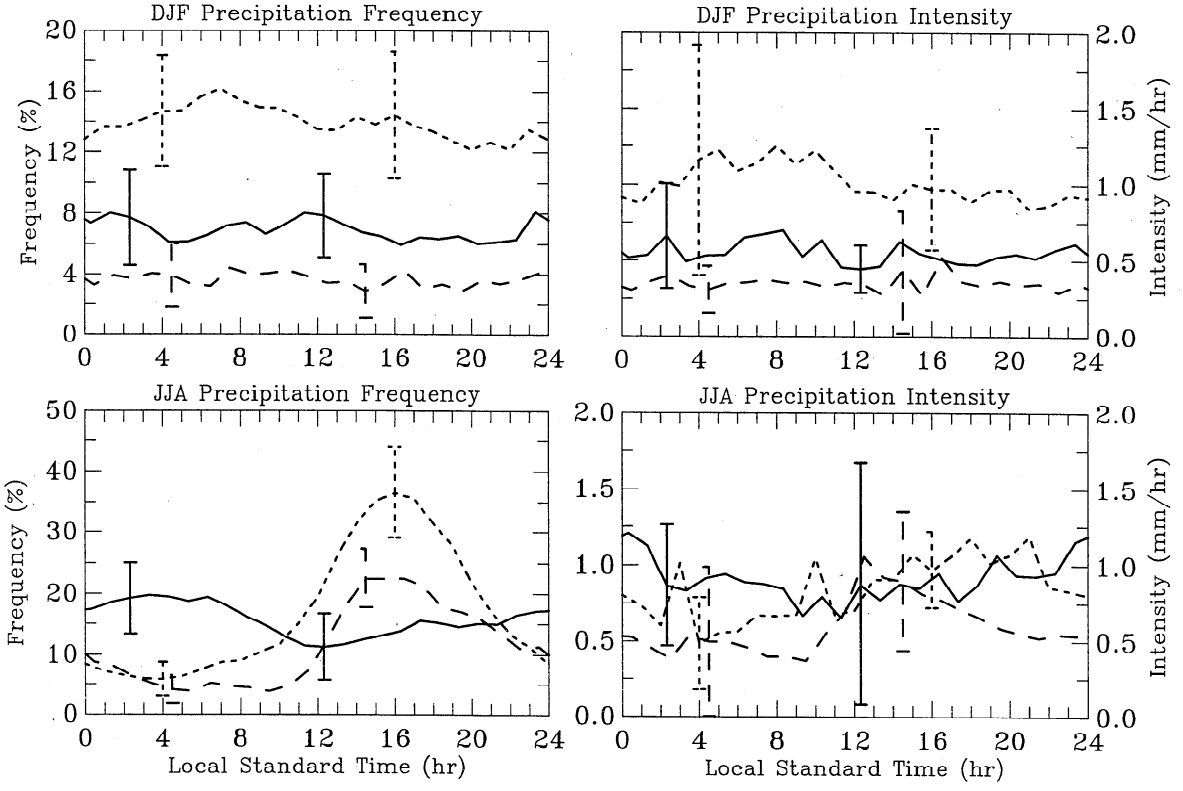

Figure 2. Mean (1963-1993) diurnal cycles of precipitation frequency and intensity in winter (DJF) and summer (JJA) at the three grid boxes marked by crosses in Figure 1: the S.E. box (82.5°W, 32°N, short-dashed curve), the central box (92.5°W, 42°N, solid curve), and the Rocky Mountain box (115°W, 37°N, long-dashed curve). The error bars represent the ±1.0 s.d. range.

with the model simulated surface solar irradiance. This approximation is acceptable for our purpose because (1) the cloud cover for July 1993 (compare Figure 19) is comparable with that during the 1985-1988 period over the southern United States and (2) the interannual variations are much smaller than the differences that we will discuss over the southern United States.

3. Observed Diurnal Cycle of Precipitation

3.1. Climatological Mean Patterns

The diurnal cycle in climatological mean precipitation (Figure 2) in winter (December-February, DJF) and summer (June-August, JJA) of precipitation frequency and intensity was averaged over the 1963-1993 period at three different grid boxes. It can be seen that diurnal variations are small in winter precipitation, while summer rainfall occurs much more frequently in the afternoon (1300-1800 LST) at the southeastern and Rocky Mountain grid boxes and more frequently from midnight to 0700 LST at the central U.S. grid box. It should be noticed that the intensity variations are relatively small and insignificant at all the three locations. In the following, we will show that these properties are representative for the regions where the grid boxes are located.

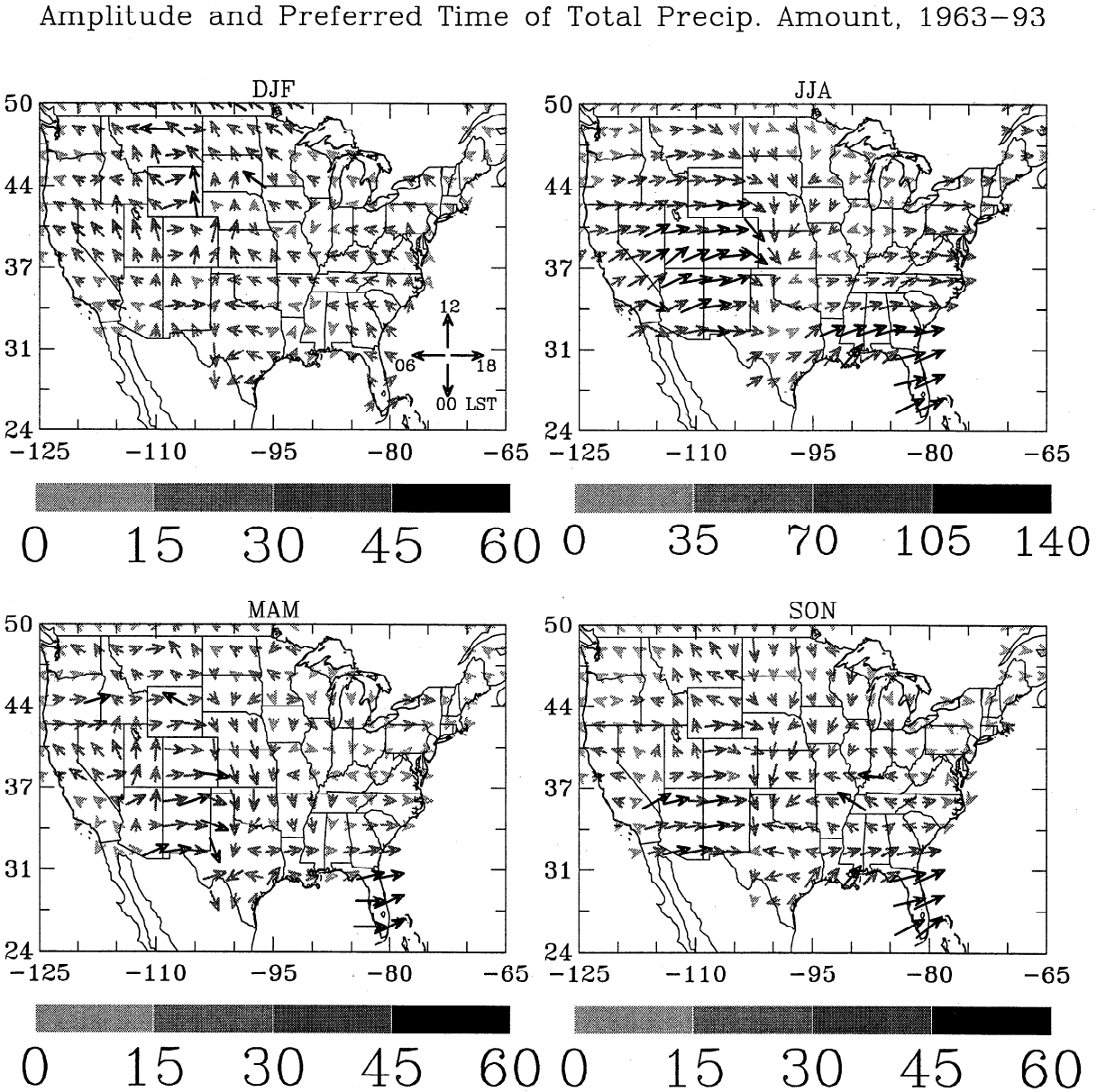

Figure 3. Vector plots of diurnal cycle of mean (1963-1993) precipitation amount. The vector length and grey levels represent the normalized amplitude in percentage (see section 2.1 for more details). The direction to which an arrow points denotes the local time at which the maximum amplitude occurs as indicated by the phase clock in the top left panel. (South = 0000 LST, West = 0600 LST, North = 1200 LST, and East = 1800 LST). For example, a vector pointing east means that the maximum amplitude occurs at 1800 LST.

Figures 3-5 show the normalized diurnal amplitude and the preferred time of occurrence for precipitation amount, frequency, and intensity (averaged over the 1963-1993 period prior to the diurnal analysis) for the four seasons. There are several observations from Figures 3 to 5.

1. The diurnal cycles of precipitation amount and frequency are very strong in summer (the maximum is over 2 times the 24-hour mean) with the preferred time between 1600 and 1800 LST over the Rocky Mountains and the Southeast and only moderate in spring (March-May, MAM) and fall (September-November, SON) over most of the country, except for Florida, where the cycles are strong in all but the winter season.

2. During spring and fall the nocturnal maximum over the region east of the Rockies and the adjacent plains is still evident, but the late afternoon maximum exists only in the very southern part of the country. There is a moderate (normalized amplitude = 15-35%) morning (0700-1100 LST) maximum in autumn precipitation over the lower Mississippi River basin and the northern Rockies.

3. Diurnal variations in winter precipitation are weak, with the normalized amplitude <30% and a maximum in the morning (0700-1100 LST) over most of the country with slightly higher peaks (mostly snowfall) over the northern states (except Washington). The nocturnal maximum over the region east of the Rockies, seen in the other seasons, does not exist in winter precipitation.

4. Diurnal variations in precipitation intensity are relatively small and less coherent in space even in summer, although the intensity tends to be slightly higher around the time of maximum frequency, and diurnal variations of precipitation amount result largely from the diurnal cycle in precipitation frequency.

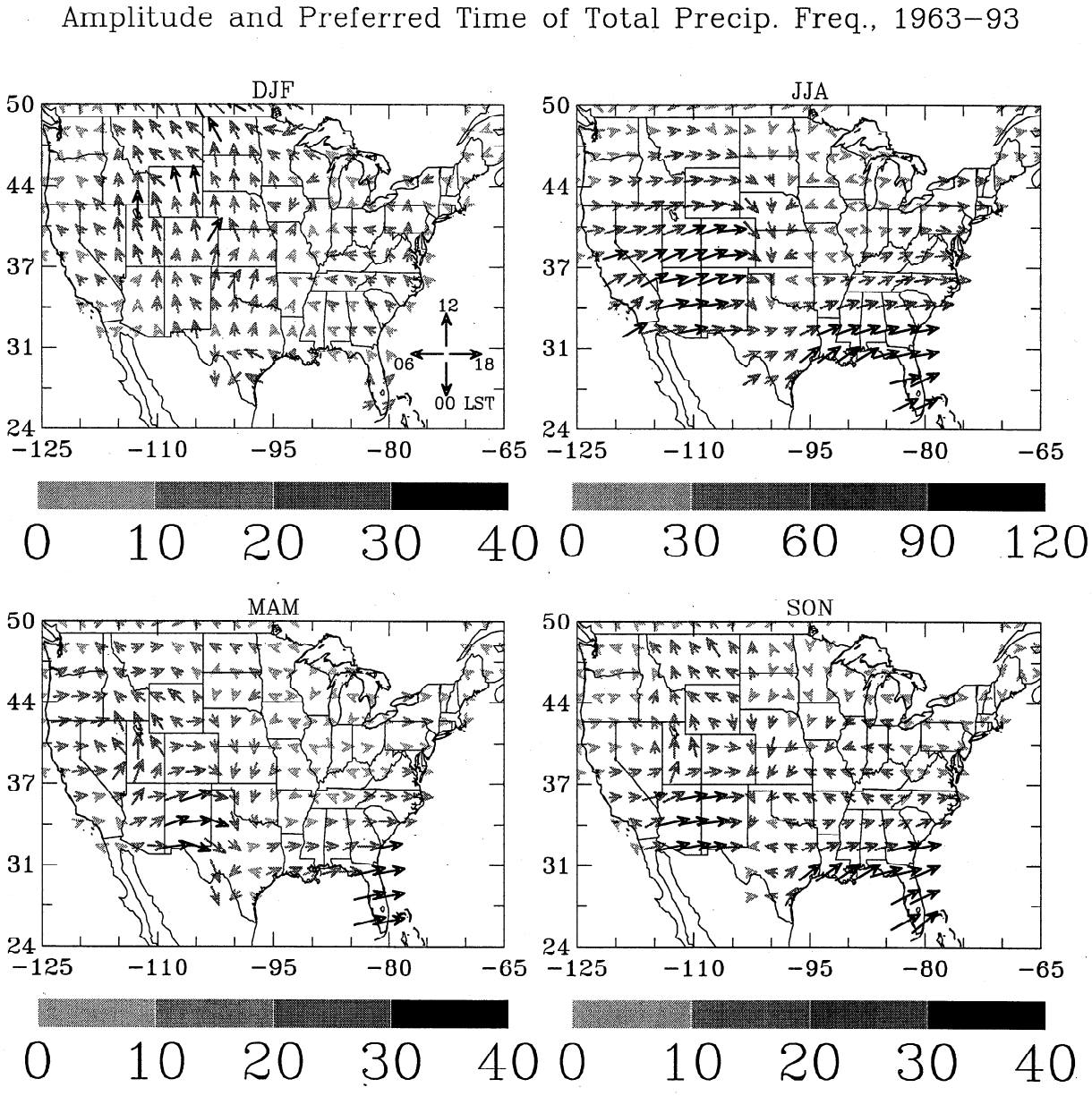

Figure 4. As for Figure 3 but for precipitation frequency.

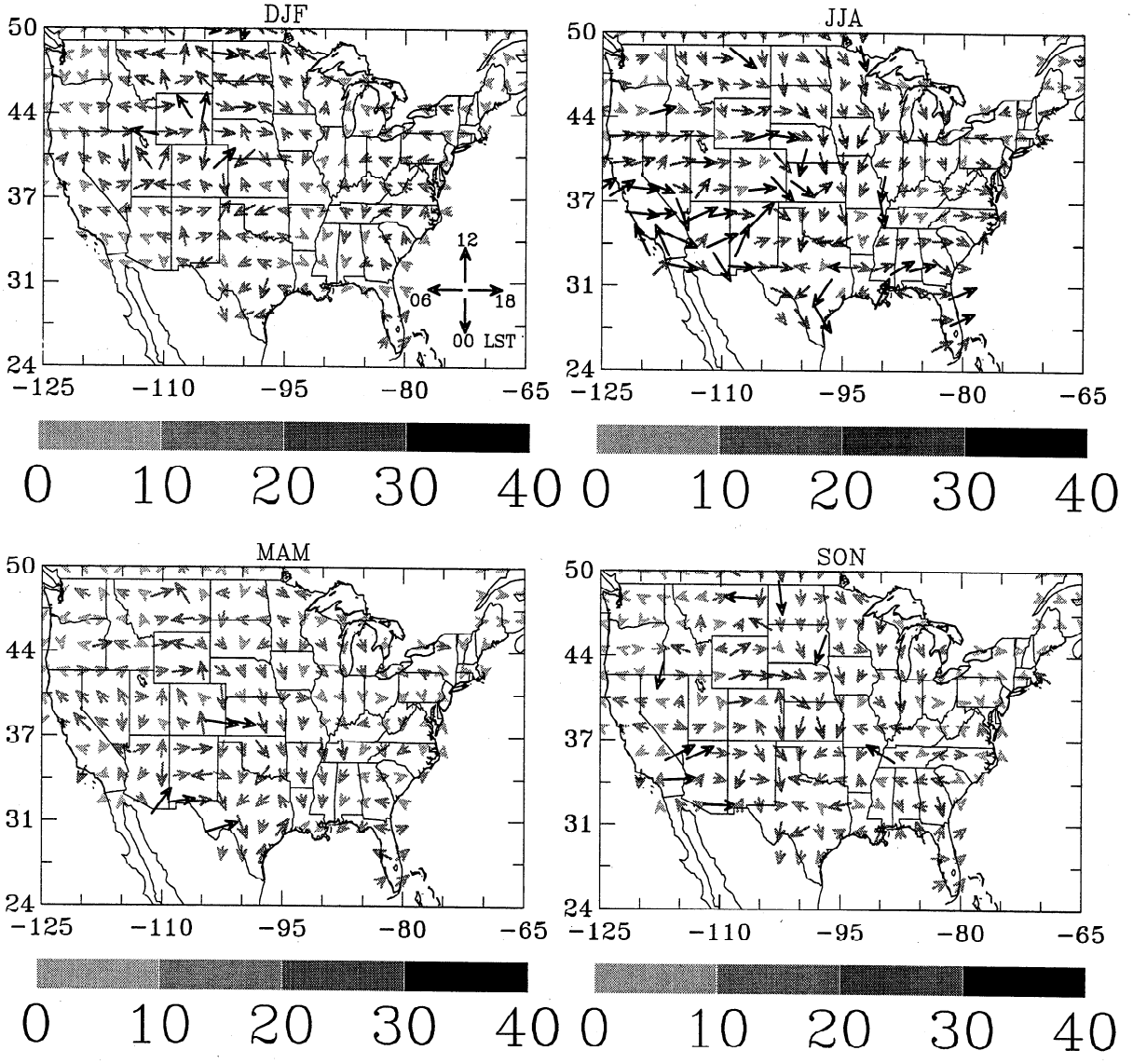

Figure 5. As for Figure 3 but for precipitation intensity.

5. There is a transition in the preferred time of precipitation from late afternoon to midnight to early morning from the Rocky Mountains to the Great Plains in all seasons except winter. The transition occurs between 105°W and 100°W and is right over the deep terrain slopes (compare Figure 1). East of about 97°W the preferred time does not change significantly across the Great Plains (0200 – 0300 LST in summer, around midnight in spring, and midnight to 0200 LST in fall).

6. Besides the region east of the Rockies, the diurnal cycles over the central United States are relatively weak all year-around.

Compared with previous studies, Figures 3-5 provide a more comprehensive picture of the mean diurnal cycle of precipitation over the United States. The broad features of Figure 4 are consistent with those derived from station data [*Wallace*, 1975; *Schwartz and Bosart*, 1979; *Riley et al.*, 1987; *Landin and Bosart*, 1989]. The preferred times shown by *Higgins et al.* [1996] appear to be 2-3 hours later over the Rockies and 2-3 hours earlier over the Southeast in comparison with Fig. 4 and the other studies.

3.2. Variability of the Diurnal Cycle of Precipitation

The standard deviations (s.d.) of the normalized amplitude and preferred time for winter and summer precipitation frequency and intensity are shown in Figure 6 (plots for precipitation amount are similar to those for the intensity). Figure 6 shows that the strong diurnal

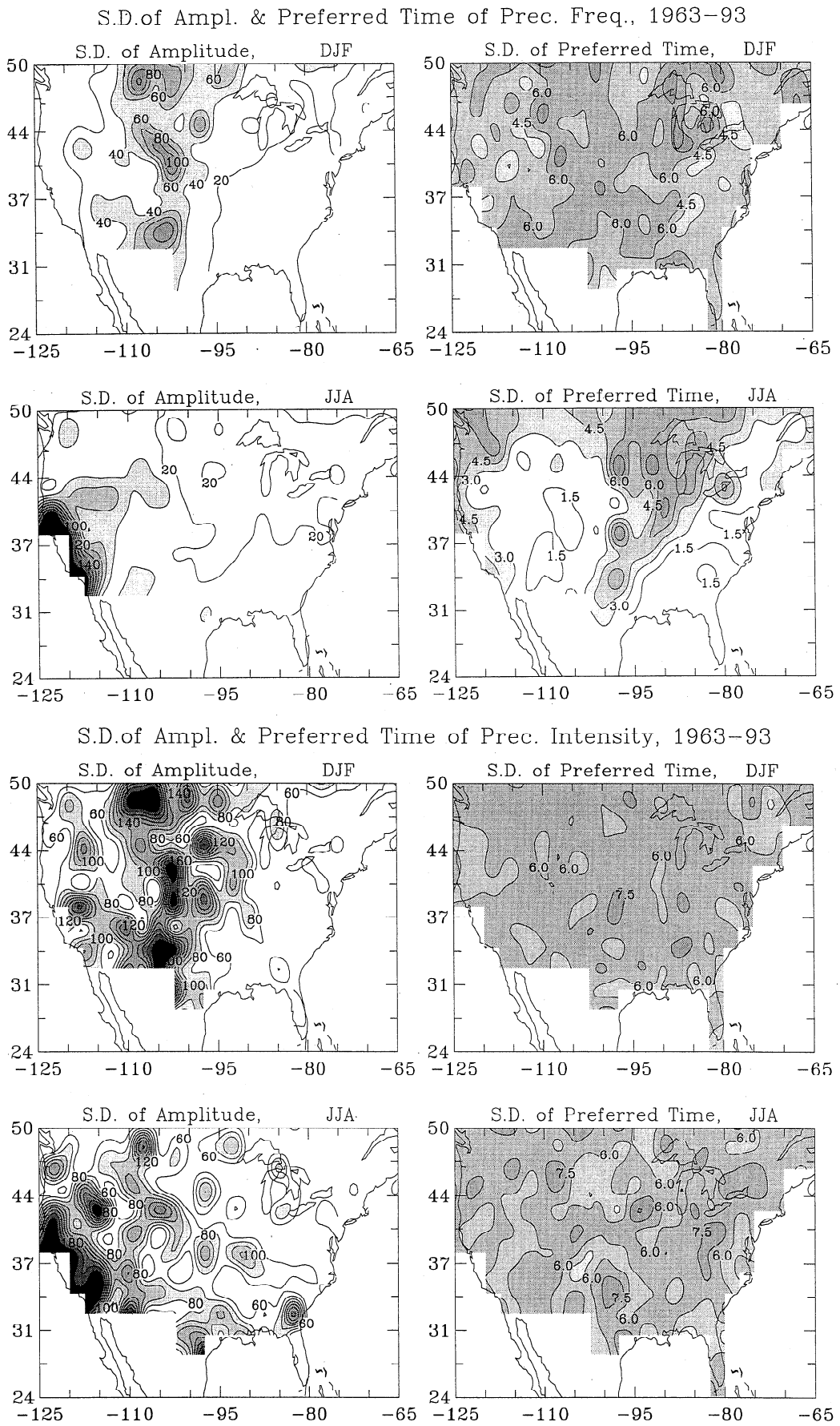

Figure 6. Standard deviations of the normalized amplitude (%) and preferred time (hour) for winter and summer precipitation frequency (a) and intensity (b) during the 1963-1993 period.

cycle in summer precipitation over the Rocky Mountains and the Southeast has small (relative to the mean) variability during the 1963-1993 period for both the amplitude and the preferred time. The diurnal cycle is relatively more variable in winter than in summer (the large numbers over California in summer are caused by the small values of 24-hour mean precipitation used in the normalization). The (normalized) intensity cycle is also more variable than the frequency cycle. These patterns suggest that the stronger the diurnal cycle, the less variable it is. For spring and fall, the s.d. plots of the amplitude are similar to that for summer, and the s.d. plots of the preferred time are comparable to that for winter.

Another way to examine the year-to-year variability is to compare those years with unusual events such as 1983, 1988, and 1993. Station records [*Dai et al.*, 1997] show that precipitation was above normal over most of the United States in the spring of 1983 and below normal in the eastern and central United States in the summer of 1983. There were severe drought conditions during the spring and summer of 1988 over the Midwest and (to a less extent) the Southeast. Summer precipitation in 1993 was well above normal in the upper

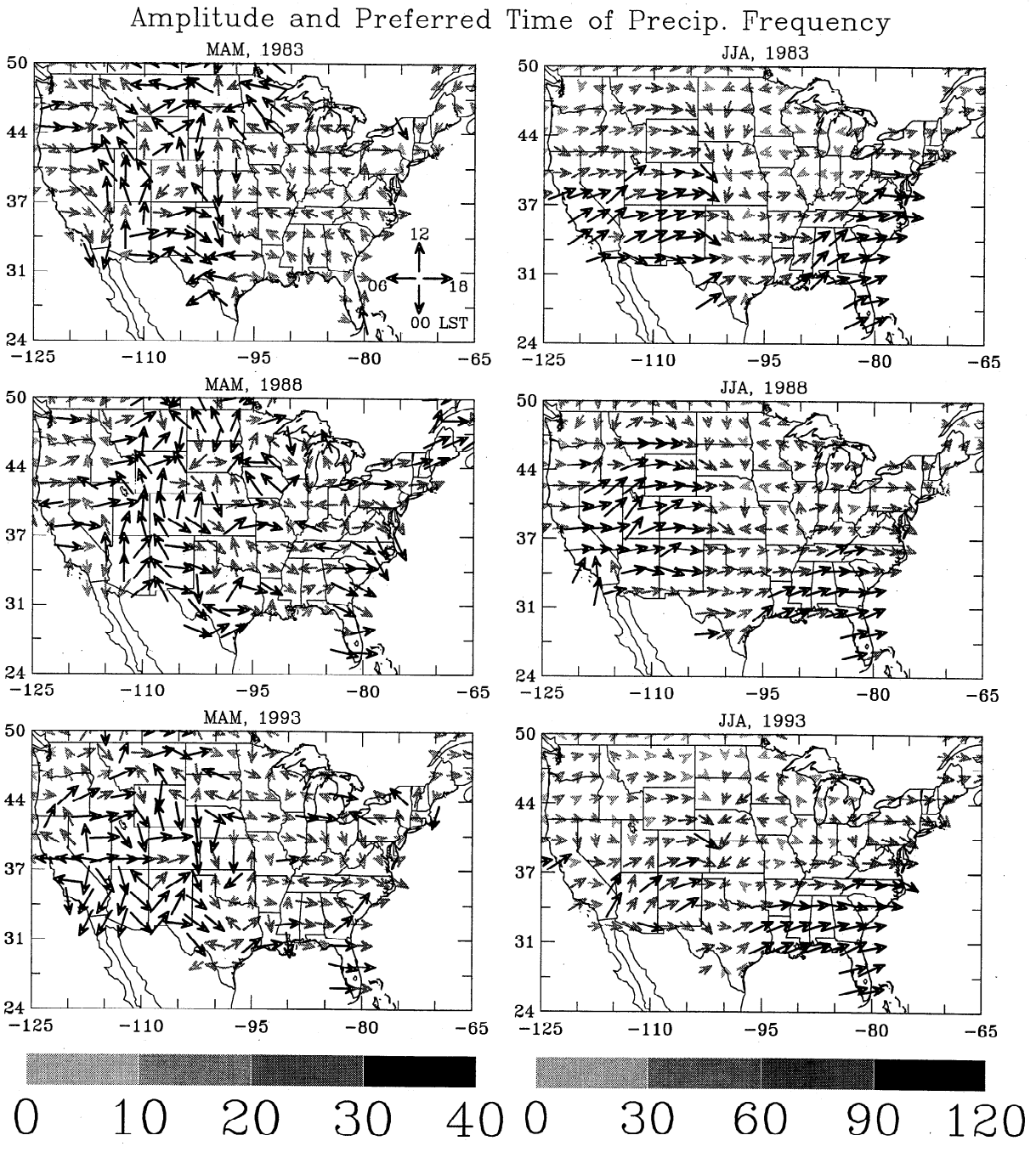

Figure 7. As for Fig. 3 but for spring (MAM) and summer (JJA) precipitation frequency in 1983, 1988, and 1993. The amplitude is normalized by the 24-hour mean of the individual years.

Mississippi River basin and below normal in the eastern United States, including Florida [*Trenberth and Guillemot*, 1996].

Figure 7 shows the diurnal cycle of precipitation frequency for the spring and summer of 1983, 1988, and 1993. To be consistent with the s.d. calculation, we normalized the amplitude using the 24-hour mean of the individual years (when the 1963-1993 mean is used for the normalization, the magnitude of the amplitude changes over the regions having large precipitation anomalies). It can be seen that while the broad patterns in summer precipitation are comparable to those of Figure 4, there are large year-to-year differences on regional scales, especially for spring precipitation. For example, over Wyoming and Utah the diurnal cycle of summer precipitation was stronger than normal in 1988 and very weak in 1993. Over the region east of the Rockies the midnight to early morning maximum was less evident in the summer precipitation of 1988. Spatial variations of the preferred time are very large for spring precipitation over the Rockies.

It should be pointed out that here we examined only the variability in the normalized (relative) amplitude. The variability in the absolute amplitude of the diurnal cycle will be larger than that for the normalized amplitude because part of the (24-hour mean) precipitation variation has been removed by the normalization.

3.3. Physical Interpretation

Here we attempt to explain the strong diurnal cycle in summer precipitation over the Rockies, the Southeast, and the region east of the Rockies by examining the diurnal variations in atmospheric static instability, the solar-heating-induced large-scale convergence in the lower troposphere, and the vertical motions in the NCEP/NCAR reanalysis. The underlying assumption is that summer precipitation over the three regions results largely from convective rainfall, which is consistent with the significant correlation between summer rainfall amount and atmospheric instability found by *Peppler and Lamb* [1989] over much of the United States. The

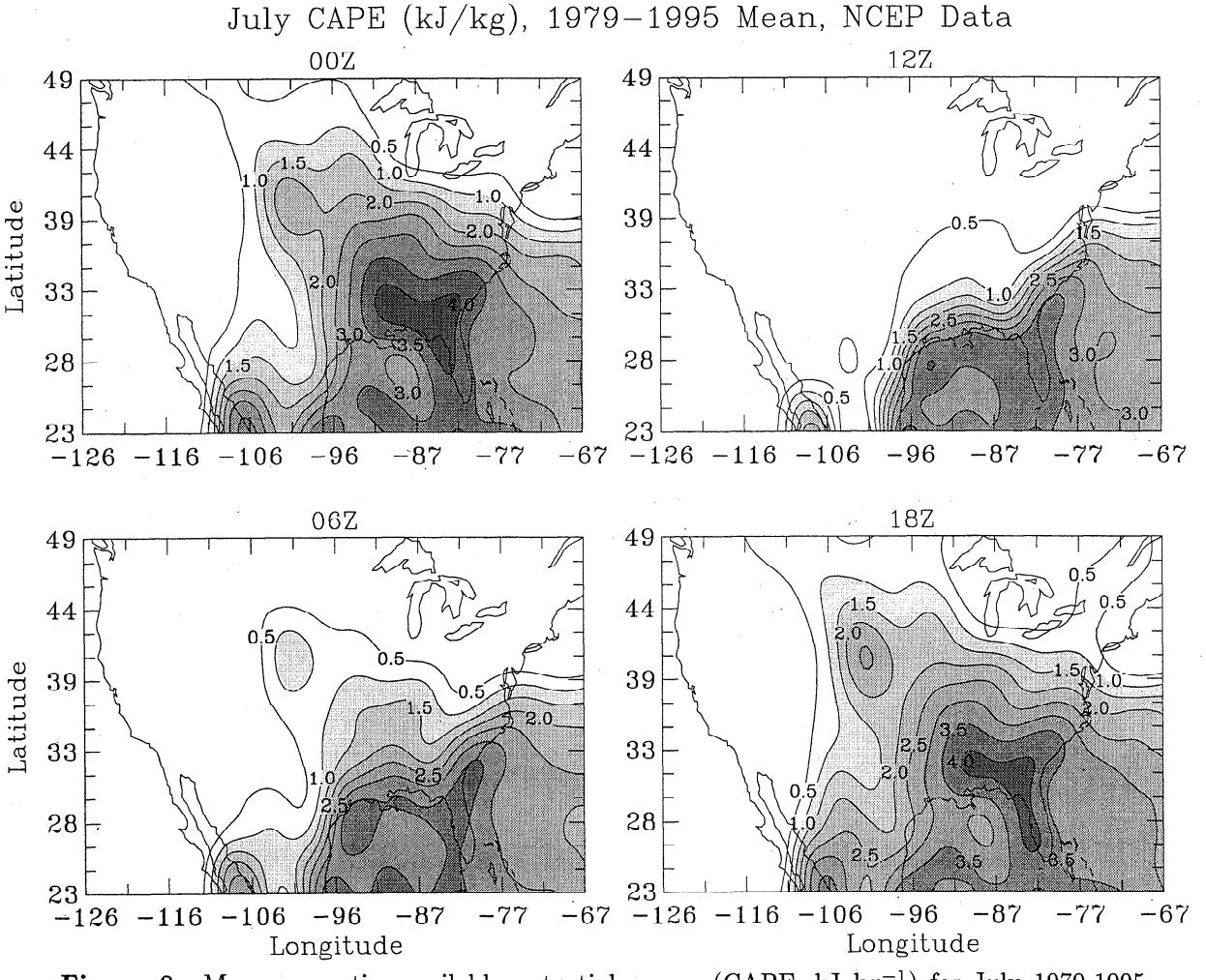

Figure 8. Mean convective available potential energy (CAPE, kJ kg^{-1}) for July 1979-1995 calculated using the temperature and humidity profiles from the 6 hourly NCEP/NCAR reanalysis (of individual years) and a pseudoadiabatic (without condensate loading) process. CAPE is slightly lower but with similar spatial patterns when a moist adiabatic (with condensate loading) is used. The CAPE for July of each year is averaged to derive the mean CAPE for July.

lack of strong diurnal variations in winter precipitation is also consistent with the assumption.

In summer, strong solar heating at the surface generates large sensible and latent heat fluxes from the surface into the lower troposphere, making the atmospheric column most favorable for convection during the afternoon. Figure 8 shows that the diurnal cycle in mean July CAPE over the United States can be described as a diurnal march of a high-CAPE (2-4 kJ kg^{-1}) tongue from the Southeast moving toward the Northwest. As a result of this, the atmosphere contains maximum CAPE during the late afternoon and early evening over the Southeast (CAPE=3.5-4.0 kJ kg^{-1}), the central United States (CAPE=2-3 kJ kg^{-1}), and the Rockies (CAPE=1-2 kJ kg^{-1}). If there were no diurnal variations in the low-level convergence, which is necessary for initiating moist convection, convective rainfall would be expected to occur most likely during the late afternoon to early evening over the three regions. Note that there is still considerable CAPE (~1 kJ kg^{-1}) in the atmosphere around midnight over the region east of the Rockies and the Great Plains. Over west of the Rockies, CAPE is low (< 0.5 kJ kg^{-1}) all day, consistent with the small diurnal cycle of precipitation in the region (Figures 3-5).

The solar heating in the atmosphere and at the surface not only makes the atmosphere conditionally unstable locally but also induces diurnal variations in pressure gradients and atmospheric circulations on both regional (such as sea breezes) and large scales [e.g., *Wallace and Hartranft*, 1969]. Figure 9 shows the diurnal and semidiurnal cycles in the summer surface pressure field over the United States and the resultant diurnal minimum divergence (maximum convergence) and the local time when the minimum occurs, as computed from equation (1). The divergence is induced largely by the

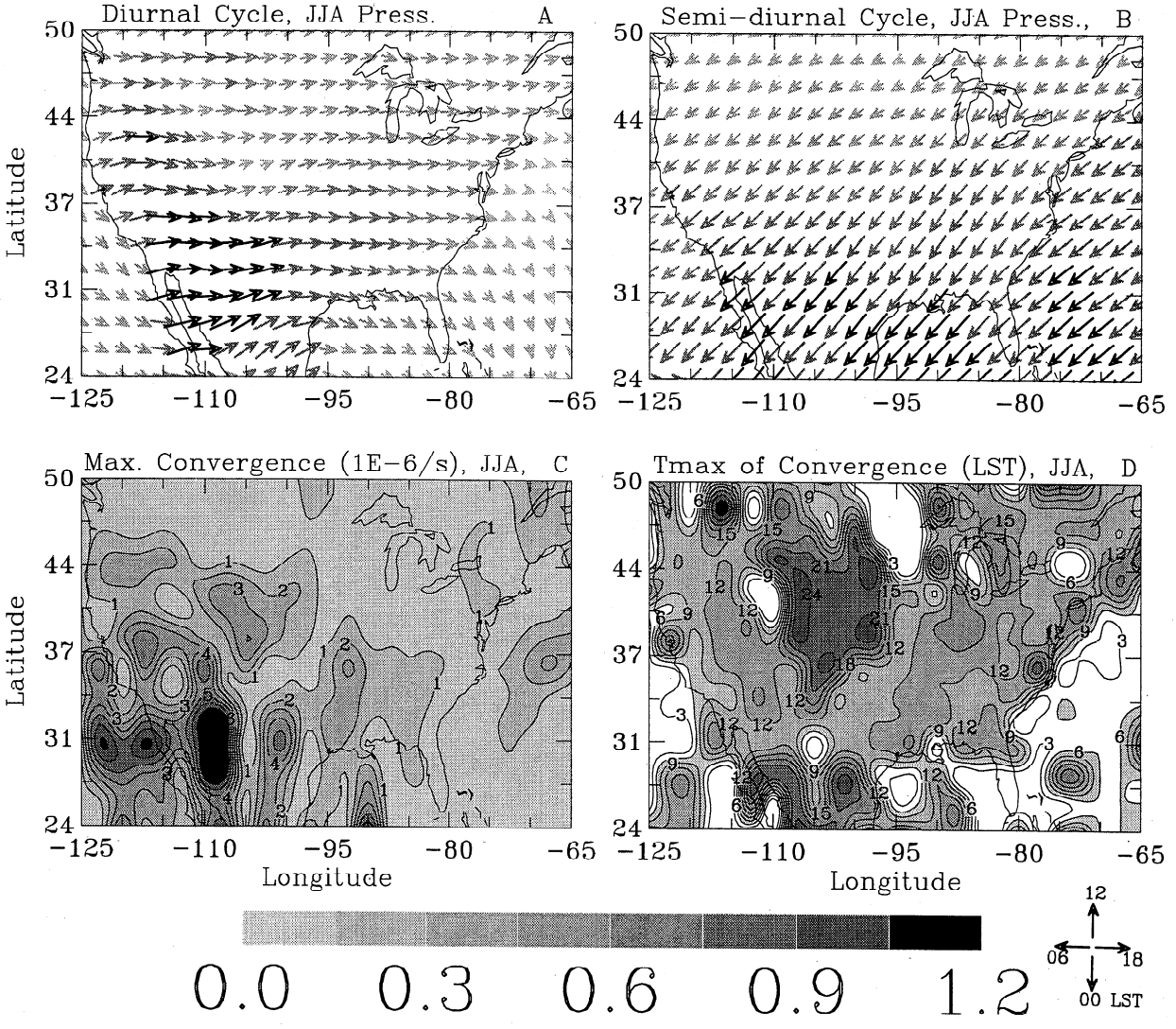

Figure 9. Vector plots (same phase clock definition as in Figure 3 except that it is the time of minimum pressure) of the (A) diurnal and (B) semidiurnal harmonics in the 1980-1994 mean field of JJA surface pressure. The vector length and grey levels (the grey bars at the bottom) represent the amplitude (mbar) of the pressure harmonics. Also shown are (C) the diurnal maximum of convergence (10^{-6} s^{-1}) induced by the two harmonics of the surface pressure and (D) the local time (hour) when the maximum convergence occurs.

surface pressure diurnal cycle with small contributions from the semidiurnal cycle. It can be seen that the pressure diurnal cycle is very strong over the western (especially, southwestern) and central United States, while the pressure semidiurnal cycle is fairly uniform zonally as part of the global-scale propagating wave. The pressure diurnal cycle reaches its minimum around 1600-1800 LST (which is close to the time (~ 1500 LST) of the second minimum of the semidiurnal cycle) over most of the United States. The spatial pattern of the amplitude of the pressure diurnal cycle follows more closely the mean cloudiness distribution [*Warren et al.*, 1986] than the contour lines of the topography (compare Figure 1), suggesting that clouds affect the diurnal cycle at the surface primarily through their modulation of the solar irradiance [*Dai et al.*, 1998].

The spatial gradient in the amplitude and the difference in the phase (after converting into universal time) of pressure fields can result in significant diurnal variations in surface divergence fields. Figure 9 shows that the pressure-induced diurnal variation of divergence is largest over the Rockies, the region east of the central Rockies, and the southern United States. The time of the diurnal maximum convergence is around 1200 LST over most of the country except for a region about 107°W-94°W and 35°N-46°N (around Kansas and Nebraska), where pressure-induced convergence reaches a maximum around late evening to midnight (or maximum divergence around noontime). When the divergence field is combined with the favorable atmospheric static stability conditions over these regions in summer (Figure 8), moist convection would be expected to occur in the afternoon to early evening over the Rockies and the Southeast and around midnight in the region east of the Rockies and the adjacent plains, as observed.

Plate 1 shows the low-level (sigma = 0.801) horizontal and vertical winds derived from the NCEP/NCAR reanalysis for the mean July conditions during the 1979-1995 period. The vertical motion of Plate 1 includes the effects of the pressure field and moist convection itself. For example, the large upward motion at 1800 UTC over the Southeast results at least partly from convection. The land-ocean contrast also induces planetary-scale circulations over the United States which are part

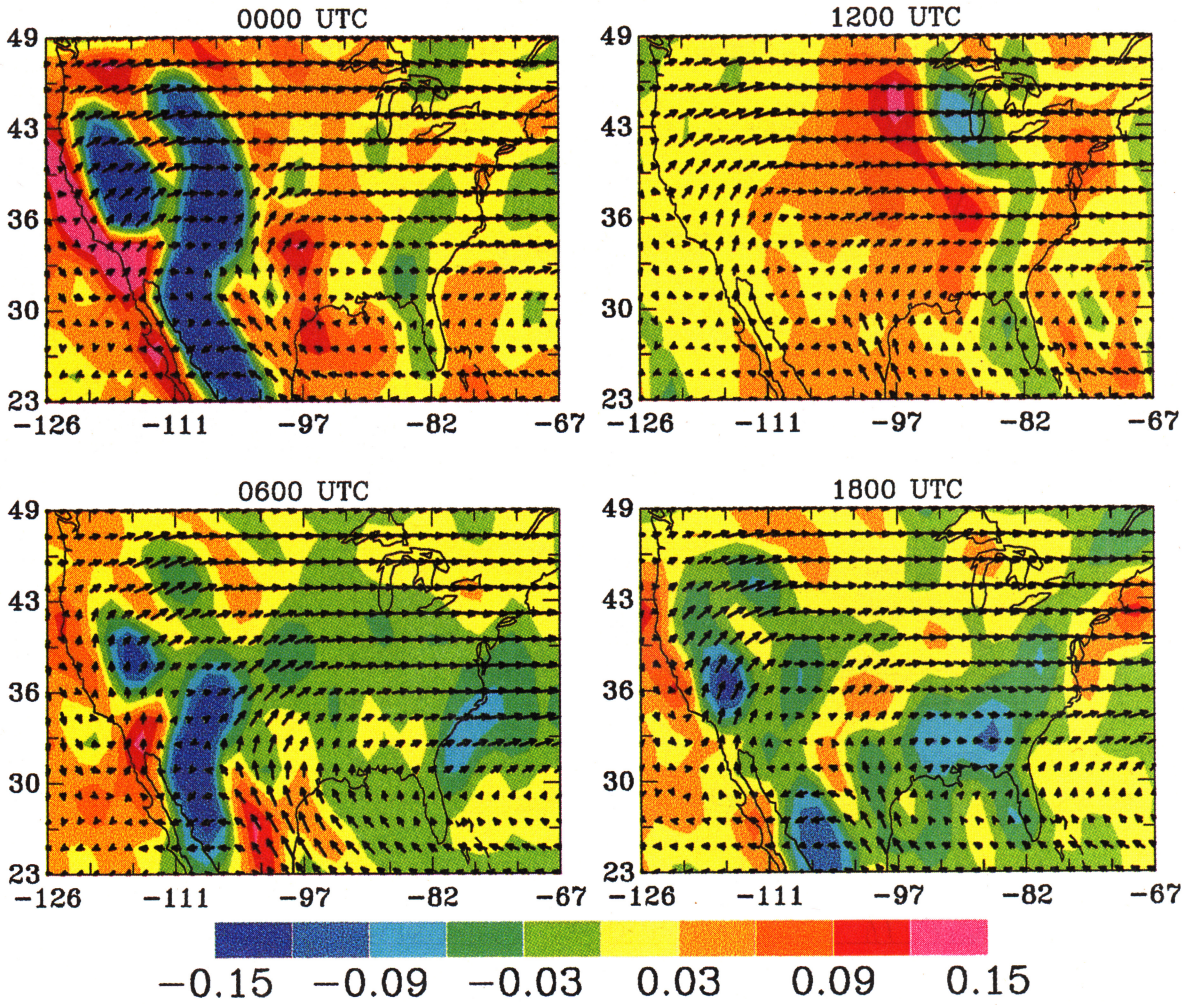

Plate 1. Horizontal winds (vectors, maximum length = 8.5 m/s) and vertical P-velocity ω (Pa/s, colored contours) at sigma=0.801 level for mean (1979-1995) July conditions derived from the NCEP/NCAR reanalysis.

of the vertical motion shown in Plate 1. For example, the continental-scale downward motion in the morning (1200 UTC) results mostly from the land-ocean circulation. Plate 1 shows that during the daytime (1800 UTC), large-scale vertical motion is unfavorable for convection in the region east of the Rockies and the adjacent plains. During the nighttime (0600 UTC), the low-level jet along the eastern slopes of the Rockies strengthens and converges into the westerlies of the higher latitudes. This creates a convergence zone from the region east of the Rockies to the Great Plains during the nighttime.

In summary, Figures 8 and 9 and Plate 1 show that over the Southeast and the Rocky Mountains there are favorable conditions during summer afternoons in both atmospheric static instability and low-level convergence so that convective rainfall occurs most frequently during the afternoon over the two regions. This is consistent with the findings of *Peppler and Lamb* [1989] who noted that the correlation between summer rainfall amount and atmospheric instability tends to be higher in the afternoon than in the morning over these two regions. Over the region east of the Rockies and the adjacent plains, where there is considerable CAPE around midnight, large-scale low-level convergence suppresses convection during the daytime and favors nighttime moist convection. The convergence arises in part from the thermally driven diurnal and semidiurnal cycles of the surface pressure field and is also closely related to the low-level jet over the eastern slopes of the Rockies. The phase transition between 105°W and 100°W over the deep terrain slopes suggests that some of the late afternoon thunderstorms over the Rockies are propagated eastward by the westerlies under favorable large-scale conditions, as we often see in summer weather over eastern Colorado. East of about 97°W the nocturnal maximum is much weaker, and the phase does not change significantly, indicating that most of the eastward propagating thunderstorms die out around 97°W. Over west of the Rockies, CAPE is too low for moist convection, which is necessary for a strong diurnal cycle in summer precipitation.

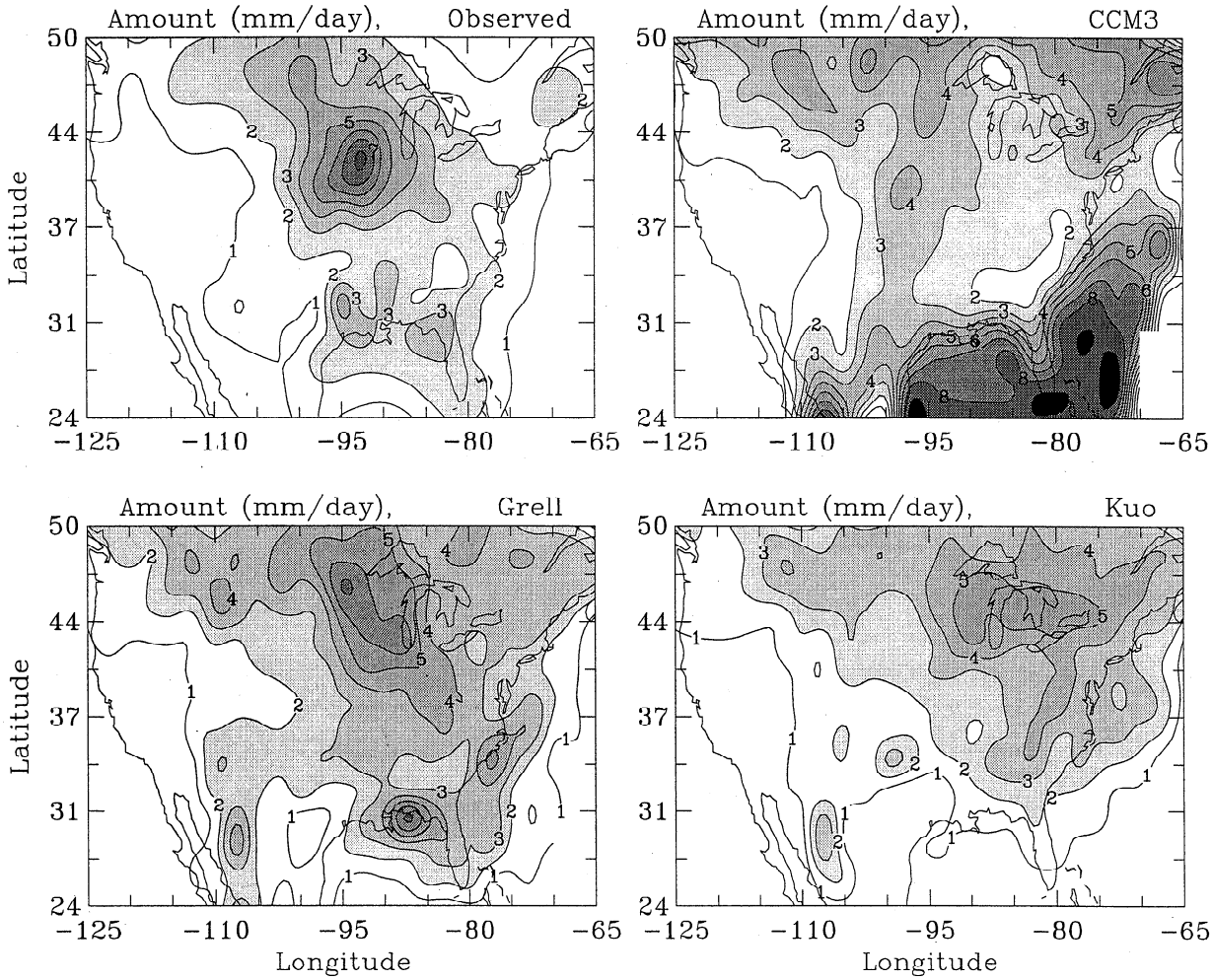

Figure 10. Observed and model simulated (with the three versions of cumulus convection schemes) total precipitation (mm/day) over the United States during the summer (JJA) of 1993.

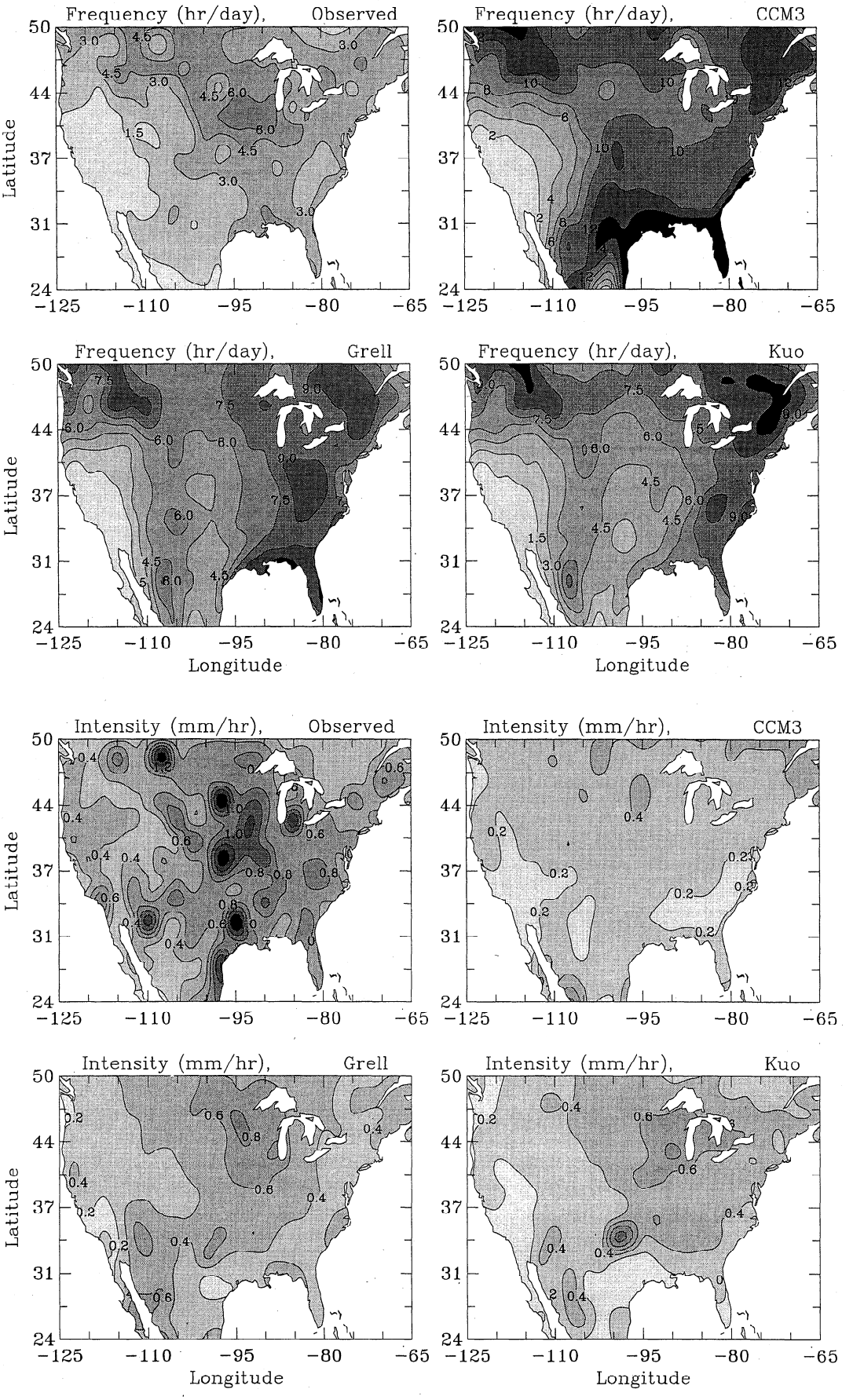

Figure 11. As for Figure 10 but for (a) precipitation frequency (hour/d) and (b) intensity (mm/h).

4. Model Simulated Diurnal Cycle of Precipitation

In this section we focus on the model-simulated diurnal cycle of 1993 summer precipitation over the United States. We first compare the model-simulated precipitation fields and precipitation diurnal cycles with observations and then diagnose the deficiencies of the model. The model was run separately, with the three different convective schemes, continuously from March 1, 1993 to 28 February 1996. The diagnostic analysis used the hourly data only from the period from June 29 to July 28, 1993 (hereinafter referred to as July 1993). The simulated diurnal cycles (in terms of the normalized or relative amplitude and phase) for the other two summers (1994 and 1995) are similar to those of 1993.

4.1. Comparison with Observations

The summer of 1993 experienced record flooding in the upper Mississippi River basin [*Kunkel et al.*, 1994; *Trenberth and Guillemot*, 1996]. Thus it is a challenge for the model to simulate the precipitation field during this period. Figure 10 compares the simulated summer precipitation of 1993 with the observed. It can be seen that the Grell scheme captures the broad patterns of the observed precipitation better than the others but still with notable differences. The high-precipitation center near the southern boundary and 108°W is likely affected by the nearby southern boundary of the model domain (compare Figure 1). The center of the storms in both the Grell and the Kuo schemes is shifted farther to the northeast compared to observations. The shift of the storm center is caused by stronger than observed southwesterlies over the Great Plains in the model with the two schemes [*Giorgi and Shields*, this issue]. The CCM3 scheme rains too much over the Southeast and too little over the upper Mississippi River basin, partly due to the weak southerly winds simulated over the Great Plains with this scheme [*Giorgi and Shields*, this issue].

Figure 11 presents the observed and model-simulated precipitation frequency and intensity for the summer of 1993. In general, the model rains too frequently with lower than observed intensity, especially when the CCM3 scheme is used. The intensity of the Grell scheme compares more favorably with the observations, while the frequency is too high over the Northeast for both the Grell and the Kuo schemes. The CCM3 scheme appears to have too much convective rainfall as a fraction of the total, while the Kuo scheme produces too little convective rainfall over the central and southeastern United States (Figure 12). Figure 13 shows that summer precipitation is episodic with sharp peaks that seldom last longer than a few hours. In that sense, the Grell scheme worked fairly well, while the CCM3 scheme produced precipitation patterns that often persisted several hours at lower than observed intensity.

Figure 14 compares the observed and model-simulated diurnal cycles of precipitation amount during the summer of 1993. There are several observations from Figure 14: (1) the CCM3 scheme produced diurnal cycles over the central and northeastern United States which are too strong and a couple of hours too early in the preferred time compared with observations; (2) both the Grell and the Kuo schemes missed the strong late afternoon maximum over the Southeast; (3) both the Grell and the Kuo schemes captured most of the midnight to early morning maximum over the region east of the Rockies and the adjacent plains; and (4) over the Rockies both the Grell and the CCM3 schemes captured the late afternoon maximum, whereas the Kuo scheme produced maximum precipitation in the evening. Plots of precipitation frequency and intensity (not shown) revealed that the simulated precipitation diurnal cycles resulted mostly from intensity diurnal variations while

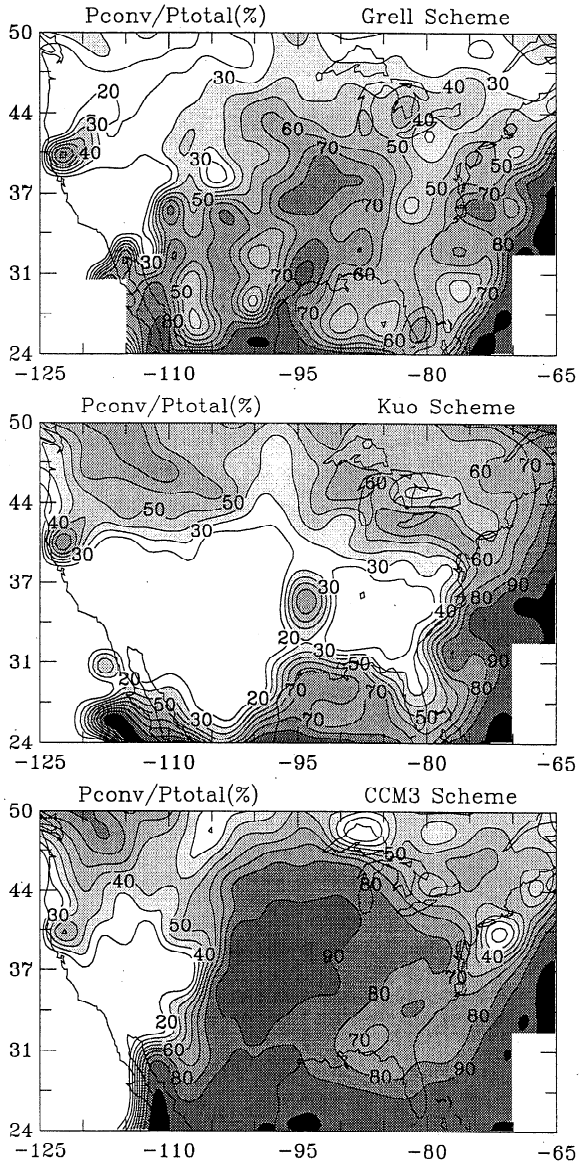

Figure 12. Simulated convective precipitation as a percentage of the simulated total precipitation by the three convection schemes.

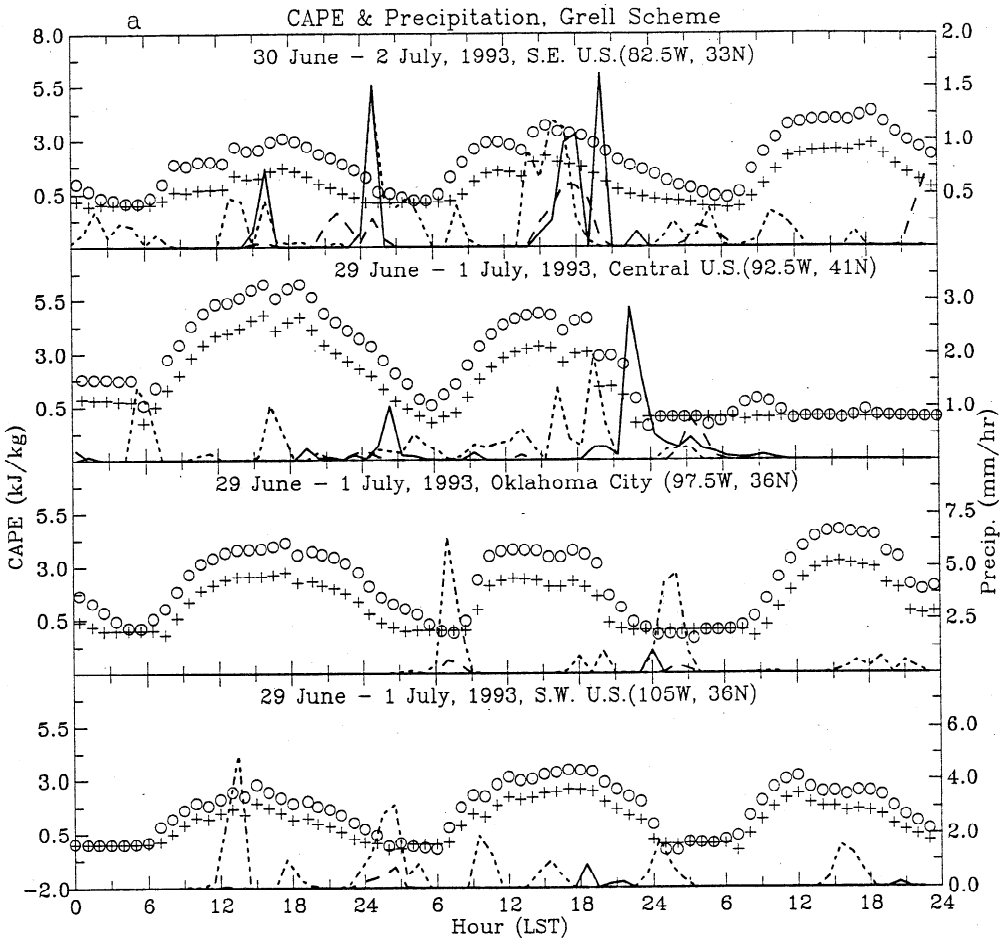

Figure 13. Observed and simulated precipitation and CAPE at four locations during the period June 29 – July 1, 1993: (a) Grell scheme and (b) CCM3 scheme. Observed total precipitation (solid curve), simulated convective precipitation (short-dashed curve), simulated large-scale precipitation (long-dashed curve) are shown. The circles and pluses are simulated CAPE derived using pseudo-adiabatic and moist adiabatic processes, respectively. The Kuo scheme produced little precipitation at the locations during the 3-day period.

the observed diurnal cycle of precipitation is largely due to frequency changes (compare Figures 3-5).

4.2. Diagnosis of Model Deficiencies

The stronger than observed diurnal cycle simulated by the CCM3 scheme over the central and much of the eastern United States is due largely to the fact that the scheme produces too much convective rainfall (Figure 12) over these regions which occurs mostly in the afternoon (compare Figure 13b). Simulated atmospheres tend to have less CAPE and weaker diurnal cycles of CAPE (Figure 15) compared with the NCEP/NCAR reanalysis (compare Figure 8). Moist convection and/or resolvable-scale precipitation events in the model apparently occur at lower static instability and too frequently (Figure 11a), thereby keeping the model atmosphere from building up high CAPE and preventing intense precipitation from occurring. The model's criteria for onset of moist convection appear to be too weak, so moist convection in the model starts too early and occurs too often with all the three schemes.

As shown in the previous section, diurnal and semidiurnal cycles of surface pressure can induce significant diurnal variations in the low-level convergence field. Figure 16 shows that the model-simulated diurnal and semidiurnal cycles of surface pressure are weak compared with observations, especially over the Southwest and for the semidiurnal cycle, which is a global propagating mode and thus more difficult to simulate by a regional model. As a result, the average diurnal cycle of the pressure-induced surface divergence is more than one order of magnitude weaker than the observed. The weak pressure diurnal variations can be traced back to the lower than observed daytime surface air temperature (Figure 17), even though the average temperatures are realistic [*Giorgi and Shields*, 1998], and further to the lower than observation-derived surface solar irradiance (Figure 18). It is evident that the model simulated cloudiness (Figure 19), which is closely related to

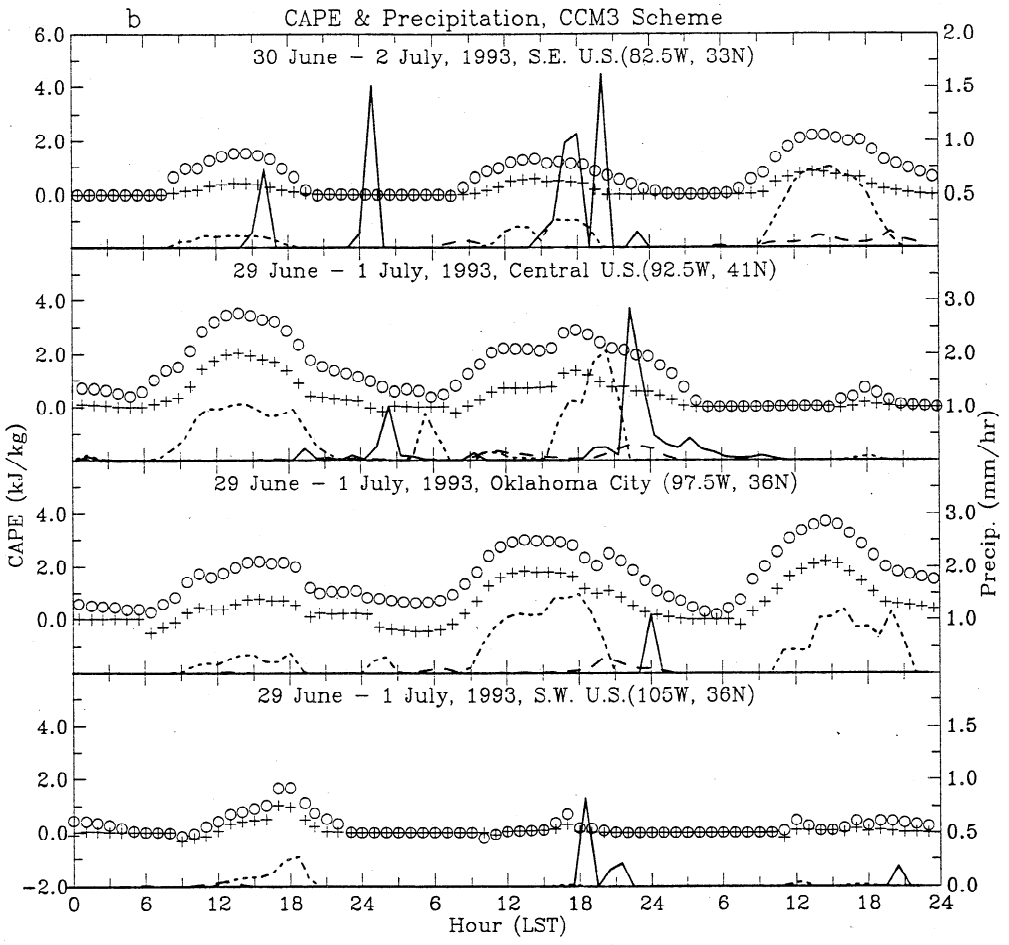

Figure 13. (continued)

the cumulus convection and resolvable-scale precipitation events in the model, is too much and also optically too thick over the southern United States, especially for the CCM3 scheme, so the surface solar irradiance is 80-160 W m^{-2} below the observation-derived fluxes around noontime over much of the southern and eastern United States (Figure 18). The model also underestimates surface solar irradiance in the northern United States even though the simulated cloud cover there is lower than observed, mainly because the model produces very high (up to 140 g m^{-2}) cloud liquid water contents in the northern United States.

Contrary to previous versions of the model, where cloud properties were diagnostically calculated from relative humidity, the cloud water content in the present version of the model is prognostically calculated via the simplified explicit moisture scheme described in section 2.3. This greatly enhances the coupling between the model hydrology and radiation but also makes the tuning for realistic clouds more difficult. *Giorgi and Shields* [this issue] and *Giorgi et al.* [this issue] show how parameters in the cloud-producing schemes can be modified to better optimize cloud-related radiation fluxes. However, the treatment of cloud-radiation processes is a difficult one, and plans are under way to improve this aspect of the model in a comprehensive fashion.

The above analysis suggests that the onset criteria for moist convection in all the three convection schemes (especially the CCM3 scheme) are too weak, so convection occurs too frequently. This leads to lower than observed precipitation intensity and too much cloudiness in the southern and eastern United States, which in turn reduces the solar radiation reaching the surface and results in smaller than observed diurnal cycles in surface temperature, surface pressure, CAPE, and low-level convergence. These reduced diurnal cycles contribute to the weak diurnal cycle of precipitation over the Southeast in the simulations with the Grell and Kuo schemes. The CCM3 scheme, on the other hand, produces too much convective rainfall over the central and eastern United States, which results in stronger than observed early afternoon maxima of precipitation over

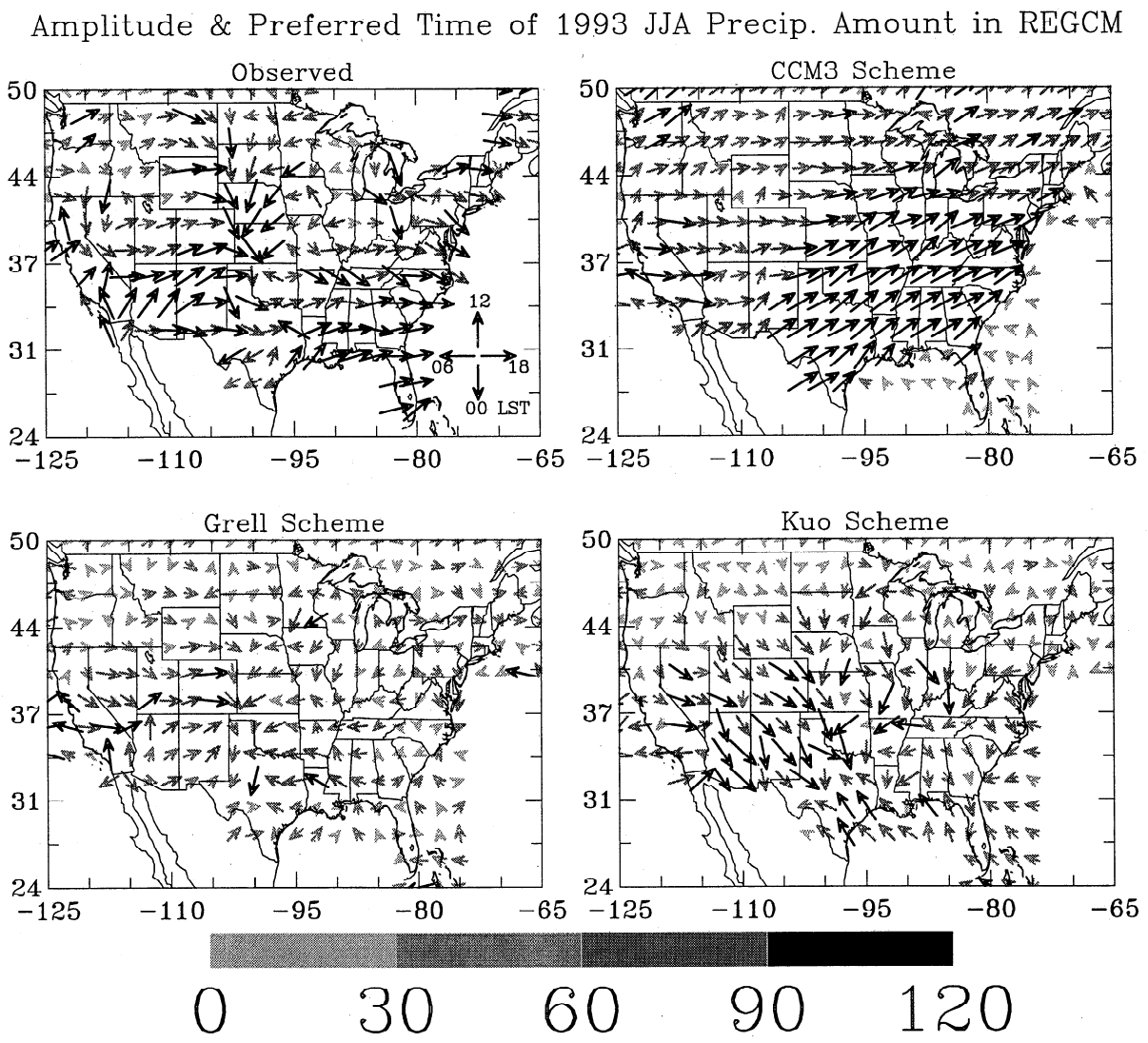

Figure 14. As for Figure 3 but for the observed and model-simulated precipitation amount for the summer 1993.

these regions. The newly implemented explicit prognostic scheme for the cloud water content also contributed to the reduced surface solar radiation in the model because of its tendency to produce high cloud liquid water contents.

It becomes clear that in order for a model to correctly simulate the diurnal variations in summer precipitation, it has to simulate the moist convection properly in terms of both frequency and intensity. As shown in the previous section, the occurrence of moist convection depends not only on the atmospheric static instability but also on the low-level convergence, which is closely related to the large-scale circulation field. Therefore in order for a cumulus convection scheme to work properly a model has to produce a realistic atmospheric circulation field, especially the convergence field, which is difficult to simulate precisely. Cumulus convection schemes may have been tuned to different levels of low-level convergence for moist convection. This is one of the reasons that even though the simulated large-scale circulations are fairly similar [*Giorgi and Shields*, this issue], the moist convection simulated by the three schemes is quite different.

5. Summary and Conclusions

We analyzed the 31-year (1963-1993) hourly precipitation data for the United States from *Higgins et al.* [1996] and presented the diurnal cycles in climatological mean precipitation amount, frequency, and intensity for the four seasons (Figures 3-5) and their year-to-year variability (Figures 6-7). Consistent with previous studies, the mean diurnal cycle in summer precipitation has a coherent spatial pattern that shows a large (nor-

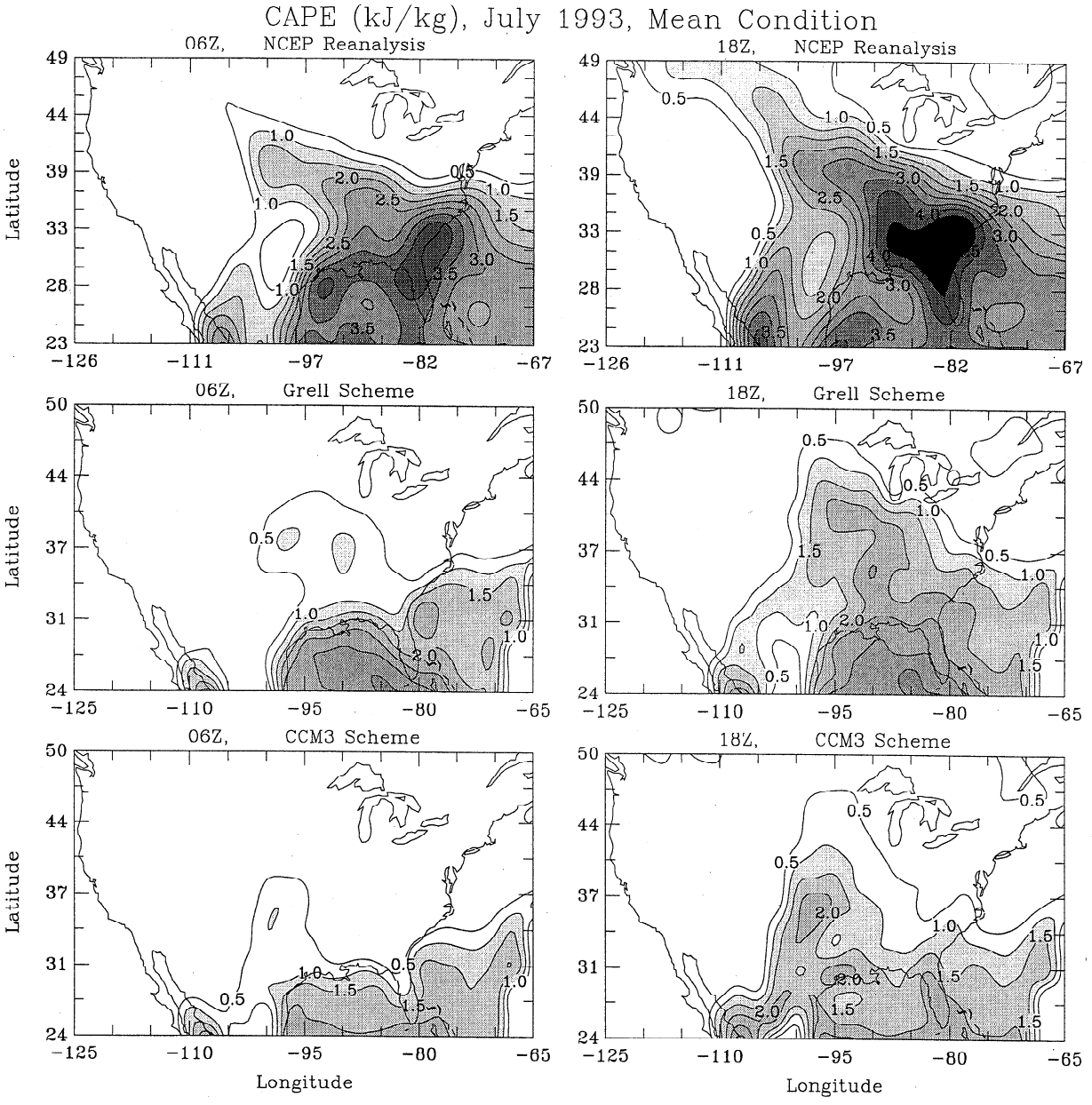

Figure 15. Daytime (1800 UTC) and nighttime (0600 UTC) CAPE for July 1993 mean conditions calculated using the temperature and humidity profiles from the 6 hourly NCEP/NCAR reanalysis (top row), simulations with the Grell scheme (middle row), and the CCM3 scheme (bottom row). A pseudoadiabatic process is used in the CAPE calculation.

malized amplitude > 100% of the 24-hour mean) late afternoon (1600-1800 LST) maximum of rainfall over the Southeast and the Rocky Mountains and a nocturnal (around midnight) maximum over the region east of the Rockies and the adjacent plains. In spring and fall the diurnal cycle of precipitation is only moderate (normalized amplitude = 15-35%) over most of the country except Florida, where the late afternoon maximum is still strong. During spring and fall the nocturnal maximum over the region east of the Rockies and the adjacent plains is still evident, but the late afternoon maximum exists only in the very southern part of the country. There is a moderate (normalized amplitude = 15-35%) morning (0700-1100 LST) maximum in fall precipitation over the lower Mississippi River basin and the northern Rockies. Diurnal variations in winter precipitation are weak, with normalized amplitude <30% and preferred time in the morning (0700-1100 LST)

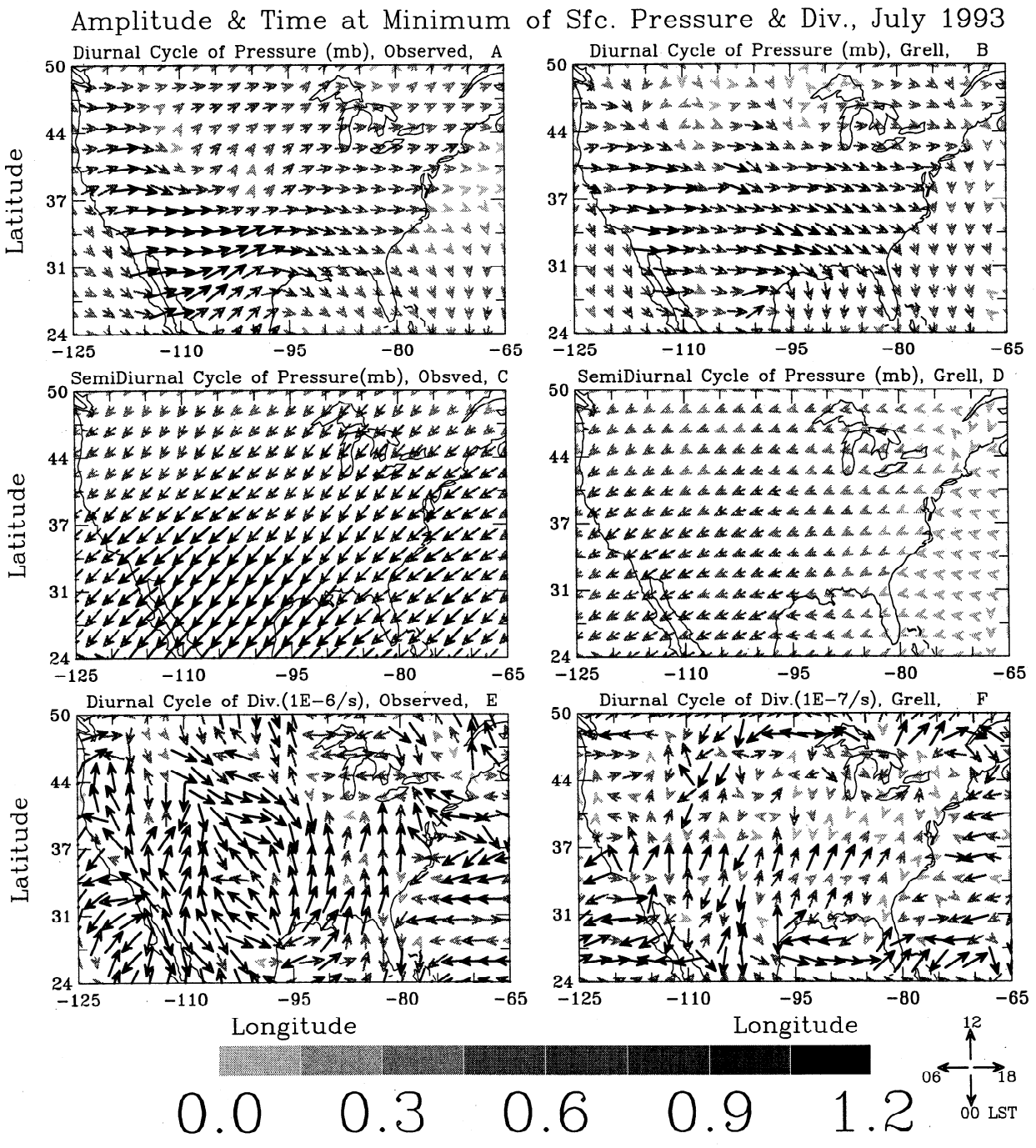

Figure 16. Vector plots of the diurnal (top row) and semidiurnal (middle row) harmonics in observed (left column) and simulated (right column) with the Grell scheme surface pressure, and the magnitude of the diurnal maximum convergence and its time of occurrence (bottom row) which result from the two pressure harmonics. The vector length and grey levels represent the amplitude (mbar) of the pressure harmonics or the magnitude of the maximum convergence (10^{-6} s^{-1} for the observed, *E*, and 10^{-7} s^{-1} for the Grell scheme, *F*). The arrow direction denotes the local time of minimum values for the pressure harmonics and of maximum values for the convergence (same clock definition as in Figure 3). Plots for the Kuo and CCM3 schemes are similar to the Grell scheme.

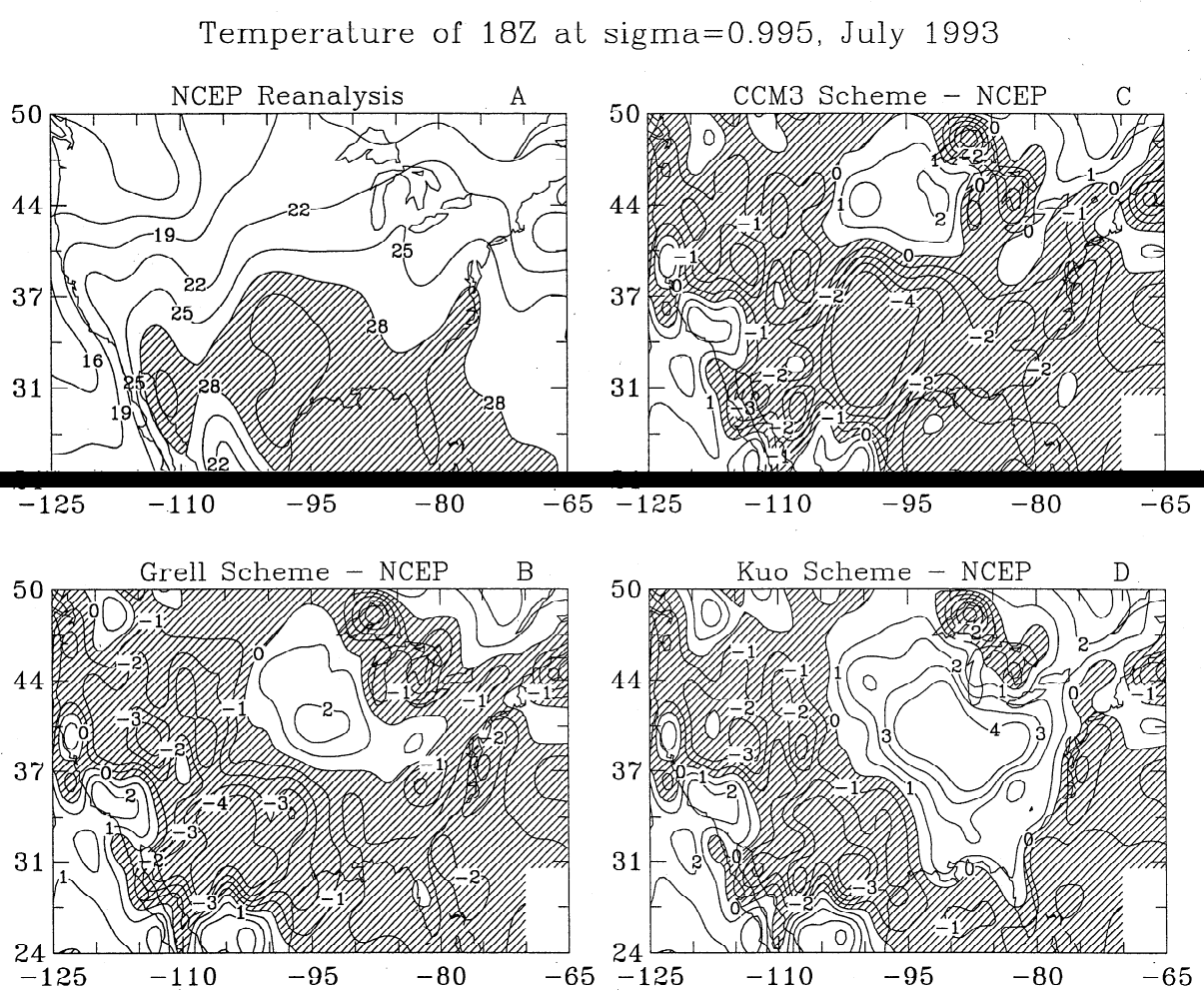

Figure 17. Surface (sigma = 0.995) air temperature at 1800 UTC for July 1993 from the NCEP/NCAR reanalysis (A, values over 28°C are hatched) and the differences between model-simulated and the reanalysis temperatures (B-D, negative values are hatched) in degrees Celsius.

over most of the country with slightly higher peaks over the northern states (except Washington). The diurnal variations of precipitation result largely from frequency variations. The diurnal cycle in precipitation intensity is relatively small and less coherent in space.

The diurnal cycle in summer precipitation has much smaller year-to-year variability than the other seasons in both the normalized amplitude and phase, implying the weaker influence of large-scale dynamics and greater importance of local effects. The spatial patterns of the diurnal cycle in the mean summer precipitation are evident even in abnormal years such 1983, 1988, and 1993. In general, the stronger the diurnal cycle, the less variable it is.

During summer months the atmosphere contains large convective available potential energy over much of the United States except west of the Rockies where the diurnal cycle of precipitation is weak. This static energy peaks in the late afternoon but is still considerable around midnight over the region east of the Rockies and the Great Plains (Figure 8). Analyses of the diurnal variations of surface pressure suggest that the thermally driven atmospheric tides tend to create a daytime low-level divergence and a nighttime low-level convergence over the region east of the Rockies and the adjacent plains. This low-level divergence cycle, which is also evident in the NCEP/NCAR reanalysis, depresses daytime convection and favors nighttime moist convection over the region east of the Rockies and the adjacent plains. The nocturnal rainfall maximum east of the Rockies is enhanced by the eastward propagation of the late afternoon thunderstorms from the Rockies under favorable low-level convergence conditions. Over the Southeast and the Rocky Mountains, both the static instability and the surface convergence favor afternoon moist convection in summer, resulting in very strong late afternoon maxima of precipitation over these regions.

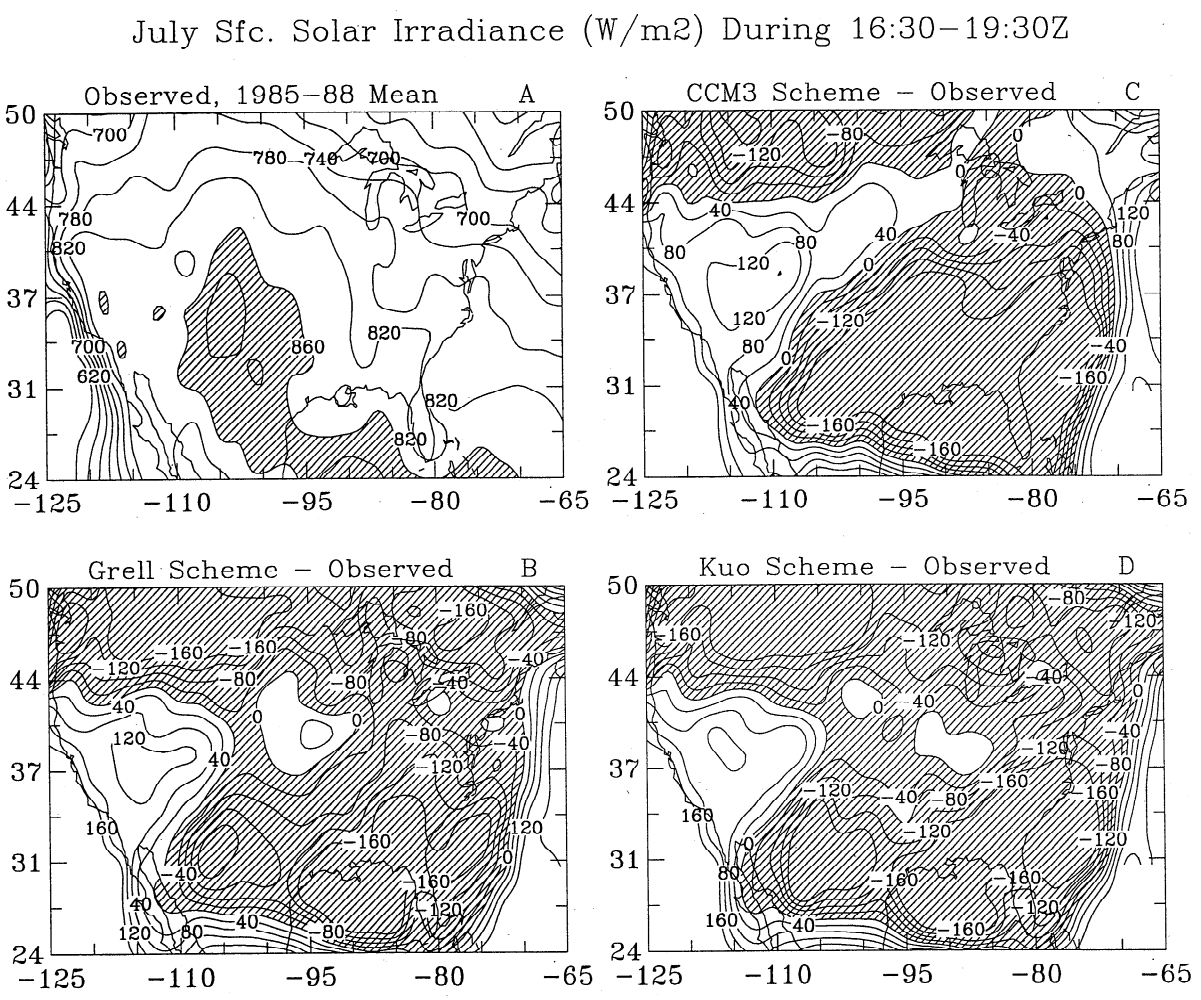

Figure 18. July noontime (1630-1930 UTC) surface solar irradiance (W m^{-2}) over the United States derived from observations (A, values over 860 W m^{-2} are hatched; data from *Zhang and Rossow* [1995]), the differences between model simulated, and the observation-derived solar irradiance (B-D, negative values are hatched). The observation-derived solar irradiance, which has year-to-year variability (s.d.) of 10-50 W m^{-2} over most of the United States, is the average value for 1985-1988.

Simulations of the diurnal cycle of precipitation for the summer of 1993 by the RegCM with the Grell scheme are reasonable except for the Southeast. The Grell and Kuo schemes captured most of the nocturnal rainfall maxima over the region east of the Rockies but failed to simulate the strong late afternoon maximum over the Southeast. Over the Rockies, both the Grell and the CCM3 schemes reproduced most of the late afternoon maximum, while the Kuo scheme produced an evening maximum. The CCM3 scheme failed to capture the nocturnal maximum and produced diurnal cycles over the central and northeastern United States that are too strong and a couple of hours earlier in phase compared with observations. Contrary to observations, much of the simulated diurnal variation of precipitation results from precipitation intensity, especially for the CCM3 and Kuo schemes.

The model tends to rain too frequently at lower than observed intensity, especially for the CCM3 scheme which had too much convective rainfall over the central and southeastern United States (*Chen et al.* [1996] also found that the precipitation frequency is too high and the intensity is too low in the NCAR Community Climate Model version 2). The model-simulated diurnal cycles in surface pressure and temperature are too weak. The model deficiencies were traced back to the problems in the model simulations of cloud cover and the cloud liquid water content. The model had too much cloud cover over the southern United States and the cloud liquid water content was too high over the northern United States, which resulted in reduced surface solar radiation and thus the diurnal cycle at the surface. The criteria for onset of moist convection in all the three schemes seem to be too weak, so moist

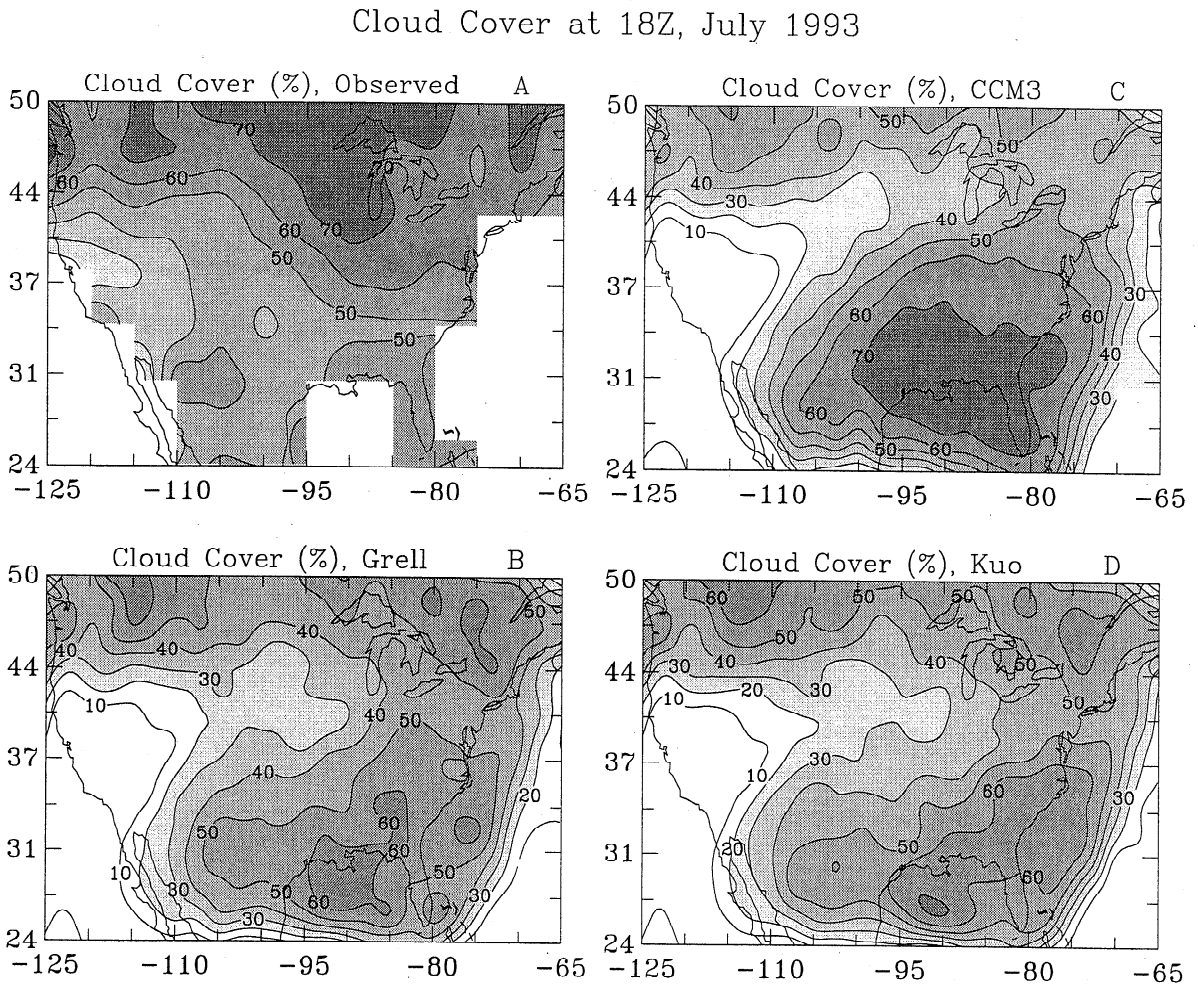

Figure 19. Observed (A) and model-simulated (B-D) cloud cover (%) at 1800 UTC for July 1993 over the United States.

convection occurs too frequently. This keeps the model atmosphere from building up high CAPE and prevents intense precipitation from occurring.

The occurrence of moist convection depends on both CAPE and the low-level convergence, and these depend on scale interactions between the regional and the continental scales. The convergence is difficult to simulate correctly and the globally propagating semidiurnal tide is poorly handled by the regional model. The RegCM simulations with the Grell and Kuo schemes had stronger than observed southwesterlies over the Great Plains which pushed the storm centers of July 1993 farther to the northeast. Our analysis suggests that for a climate model to correctly simulate the diurnal cycle in summer precipitation, it has to (1) properly simulate the regional and large-scale circulations, especially the low-level convergence field; (2) produce realistic cloud cover evolution and cloud optical thickness so that the diurnal cycle at the surface can be captured correctly; and (3) generate subgrid moist convection at the proper frequency and intensity so that the model atmosphere can maintain correct CAPE.

Climate models are usually tuned to produce the correct (monthly) mean amount of precipitation, but it is evident that they often get this right for the wrong reason. It seems that a necessary (but not sufficient) condition is to be able to simulate the diurnal cycle and the correct balance between intensity and frequency of occurrence. We recommend that more attention should be devoted to this aspect in model evaluation.

Acknowledgments. We thank A. D. Del Genio for his stimulating comments on moist convection, B. Ye for providing the code for CAPE calculations, W. Higgins et al. for providing the precipitation data set, John Wu and S. Schubert for the surface pressure data set, and Y. Zhang and Bill Rossow for the surface solar flux data. Thanks also to Doug Lindholm, Dave Stepaniak, Tim Hoar, Dennis Shea, Liz Rothney, and C. Shields for their computer or data set assistance. A. Dai is supported by a NOAA Postdoctoral Program in Climate and Global Change fellowship, administered by the University Corporation for Atmospheric Research. The National Center for Atmospheric Research is sponsored by the National Science Foundation.

References

Anthes, R. A., E. Y. Hsie, and Y. H. Kuo, Description of the Penn State/NCAR Mesoscale Model Version 4 (MM4). *NCAR Tech. Note, NCAR/TN-282+STR*, 66 pp., Natl. Cent. for Atmos. Res., Boulder, Colo., 1987.

Arakawa, A., and W. H. Schubert, Interaction of a cumulus cloud ensemble with the large scale environment, I, *J. Atmos. Sci., 31*, 674-701, 1974.

Balling, R. C., Jr., Warm season nocturnal precipitation in the Great Plains of the United States. *J. Clim. Appl. Meteorol., 24*, 1383-1387, 1985.

Bleeker, W., and M. J. Andre, On the diurnal variation of precipitation, particularly over central U.S.A., and its relation to large-scale orographic circulation systems, *Q. J. R. Meteorol. Soc., 77*, 260-271, 1951.

Burpee, R. W., Peninsula scale surface convergence and area averaged rainfall in South Florida, *Mon. Weather Rev., 107*, 852-860, 1979.

Chapman, S., and R. S. Lindzen, *Atmospheric Tides*, 200 pp., D. Reidel, Norwell, Mass., 1970.

Chen, M., R. E. Dickinson, X. Zeng, and A. N. Hahmann, Comparison of precipitation observed over the continental United States to that simulated by a climate model, *J. Clim., 9*, 2233-2249, 1996.

Dai, A., I. Y. Fung, and A. D. Del Genio, Surface observed global land precipitation variations during 1900-88, *J. Clim., 10*, 2943-2962, 1997.

Dai, A., K. E. Trenberth, and T. R. Karl, Effects of clouds, soil moisture, precipitation and water vapor on diurnal temperature range, *J. Clim.*, in press, 1998.

Deser, C., and C. A. Smith, Diurnal and semidiurnal variations of the surface wind field over the tropical Pacific Ocean, *J. Clim., 11*, 1730-1748, 1998.

Easterling, D. R., and P. J. Robinson, The diurnal variations of thunderstorm activity in the United States, *J. Clim. Appl. Meteorol., 24*, 1048-1058, 1985.

Englehart, P. J., and A. V. Douglas, A statistical analysis of precipitation frequency in the conterminous United States, including comparisons with precipitation totals, *J. Clim. Appl. Meteorol., 24*, 350-362, 1985.

Fu, R., A. D. Del Genio, and W. B. Rossow, Influence of ocean surface conditions on atmospheric vertical thermodynamic structure and deep convection, *J. Clim., 7*, 1092-1108, 1994.

Giorgi, F., and C. Shields, Tests of precipitation parameterizations available in the latest version of the NCAR regional climate model (RegCM), *J. Geophys. Res.*, this issue.

Giorgi, F., Y. Huang, K. Nishizawa, and C. Fu, A seasonal cycle simulation over eastern Asia and its sensitivity to radiative transfer and surface processes, *J. Geophys. Res.*, this issue.

Grell, G. A., Prognostic evaluation of assumptions used by cumulus parameterizations, *Mon. Weather Rev., 121*, 764-787, 1993.

Haurwitz, B., and A. D. Cowley, The diurnal and semidiurnal barometric oscillations, global distribution and annual variation, *Pure Appl. Geophys., 102*, 193-222, 1973.

Hering, W. S., and T. R .Borden Jr., Diurnal variations in the summer wind field over the central United States, *J. Atmos. Sci., 19*, 81-86, 1962.

Higgins, R. W., J. E. Janowiak, and Y.-P. Yao, A gridded hourly precipitation database for the United States (1963-1993), in *NCEP/Climate Prediction Center ATLAS No. 1*, 47 pp., U.S. Dep. of Comm., Washington, D. C., 1996.

Holton, J. R., *Introduction to Dynamic Meteorology*, 391 pp., 2nd ed., Academic, San Diego, Calif., 1979.

Hsie, E.Y., R. A. Anthes, and D. Keyser, Numerical simulation of frontogenesis in a moist atmosphere, *J. Atmos. Sci., 41*, 2581-2594, 1984.

Kalnay, E., et al., The NCEP/NCAR 40-year reanalysis project, *Bull. Am. Meteorol. Soc., 77*, 437-471, 1996.

Kiehl, J. T., J. J. Hack, G. B. Bonan, B. A. Boville, B. P. Briegleb, D. L. Williamson, and P. J. Rasch, Description of the NCAR Community Climate Model (CCM3), *NCAR Tech. Note, NCAR/TN-420+STR*, 152 pp., Natl. Cent. for Atmos. Res., Boulder, Colo., 1996.

Kunkel, K.E., S. A. Changnon, and J. R. Angel, Climatic aspects of the 1993 Upper Mississippi River basin flood, *Bull. Am. Meteorol. Soc., 75*, 811-822, 1994.

Landin, M. G., and L. F. Bosart, The diurnal vaiation of precipitation in California and Nevada, *Mon. Weather Rev., 117*, 1801-1816, 1989.

Lindzen, R. S., Thermally driven diurnal tide in the atmosphere, *Q. J. R. Meteorol. Soc., 93*, 18-42, 1967.

Lucas, C., E. J. Zipser, and M. A. LeMone, Convective available potential energy in the environment of oceanic and continental clouds: Correction and comments, *J. Atmos. Sci., 51*, 3829-3830, 1994.

Nicolini, M., K. M. Waldron, and J. Paegle, Diurnal oscillations of the low-level jets, vertical motion, and precipitation: a model case study, *Mon. Weather Rev., 121*, 2588-2610, 1993.

Peppler, R. A., and P. J. Lamb, Tropospheric static stability and central North American growing season rainfall, *Mon. Weather Rew., 117*, 1156-1180, 1989.

Pitchford, K. L., and J. London, the low level jet as related to nocturnal thunderstorms over Midwest United States, *J. Appl. Meteorol., 1*, 43-47, 1962.

Reiter E. R., and M. Tang, Plateau effects on diurnal circulation patters, *Mon. Weather Rev., 112*, 638-651, 1984.

Riley, G. T., M. G. Landin, and L. F. Bosart, The diurnal variability of precipitation across the Central Rockies and adjacent Great Plains, *Mon. Weather Rev., 115*, 1161-1172, 1987.

Rossow, W. R., and Y.-C. Zhang, Calculation of surface and top-of-atmosphere radiative fluxes from physical quantities based on ISCCP data sets, 2, validation and first results, *J. Geophys. Res., 100*, 1167-1197, 1995.

Schubert, S., et al., A multiyear assimilation with the GEOS-1 system: overview and results, *NASA Tech. Memo. 104606*, vol.6, 183pp., Data Assilimation Off., NASA Goddard Space Flight Cent., Greenbelt, Md., 1995.

Schwartz, B. E., and L. F. Bosart, The diurnal variability of Florida rainfall, *Mon. Weather Rev., 107*, 1535-1545, 1979.

Trenberth, K. E., Surface atmospheric tides in New Zealand, *N. Z. J. Sci., 20*, 339-356, 1977.

Trenberth, K. E., and C. J. Guillemot, Physical processes involved in the 1988 drought and 1993 floods in North America, *J. Clim., 9*, 1288-1298, 1996.

Trenberth, K. E., and C. J. Guillemot, Evaluation of the atmospheric moisture and hydrological cycle in the NCEP/NCAR reanalysis, *Clim. Dyn., 14*, 213-231, 1998.

Tucker, D. F., Diurnal precipitation variations in south-central New Mexico, *Mon. Weather Rev., 121*, 1979-1991, 1993.

Wallace, J. M., Diurnal variations in precipitation and thunderstorm frequency over the conterminous United States, *Mon. Weather Rev., 103*, 406-419, 1975.

Wallace, J. M., and F. R. Hartranft, Diurnal wind variations, surface to 30 kilometers, *Mon. Weather Rev., 97*, 446-455, 1969.

Warren, S. G, C. J. Hahn, J. London, R. M. Chervin, and R. L. Jenne, Global Distribution of Total Cloud Cover and Cloud Type Amount Over Land, *NCAR Tech. Notes,*

NCAR/TN-272+STR, 229 pp., Natl. Cent. for Atmos. Res., Boulder, Colo., 1986.

Williams, E., and N. Renno, An analysis of the conditional instability of the tropical atmosphere, *Mon. Weather Rev., 121*, 21-36, 1993.

Wilson, C. A. and J. F. B. Mitchell, Diurnal variation and cloud in a general circulation model, *Q. J. R. Meteorol. Soc., 112*, 347-369, 1986.

Wu, J., A. da Silva, and S. Schubert, Fifteen years (1980-1994) of three hourly surface pressure from GEOS-1 reanalysis, *Tech. Note*, Data Assilimation Off., NASA Goddard Space Flight Cent., Greenbelt, Md., 1997.

Zhang, G. J., and N. A. McFarlane, Sensitivity of climate simulations to the parameterization of cumulus convection in the Canadian Climate Centre general circulation model, *Atmos. Ocean, 33*, 407-446, 1995.

Zhang, Y.-C., W. B. Rossow, and A. A. Lacis, Calculation of surface and top-of-atmosphere radiative fluxes from physical quantities based on ISCCP data sets, 1, method and sensitivity to input uncertainties, *J. Geophys. Res., 100*, 1149-1165, 1995.

A. Dai and K. E. Trenberth, National Center for Atmospheric Research, P.O. Box 3000, Boulder, CO 80307. (e-mail: adai@ucar.edu; trenbert@ucar.edu)

F. Giorgi, Physics of Weather and Climate Group, The Abdus Salam International Centre for Theoretical Physics, P.O. Box 586, 34100 Trieste, Italy. (e-mail: giorgi@ictp.trieste.it)

(Received February 27, 1998; revised August 14, 1998; accepted August 17, 1998.)